heritage

MDPI

Article

Portable X-ray Fluorescence Analysis of Levantine and Schematic Art Pigments from the River Vero Shelters (Huesca, NE Spain)

Pablo Martín-Ramos [1,2,*], José Antonio Cuchí-Oterino [3] and Manuel Bea-Martínez [4]

[1] Instituto Universitario de Investigación en Ciencias Ambientales de Aragón (IUCA), EPS, University of Zaragoza, Carretera de Cuarte s/n, 22071 Huesca, Spain
[2] Advanced Materials Laboratory, ETSIIAA, University of Valladolid, Avenida de Madrid 44, 34004 Palencia, Spain
[3] Instituto Universitario de Investigación en Ingeniería de Aragón (i3A), EPS, University of Zaragoza, Carretera de Cuarte s/n, 22071 Huesca, Spain
[4] P3A Group, Departamento de Ciencias de la Antigüedad, Facultad de Filosofía y Letras—Instituto Universitario de Investigación en Patrimonio y Humanidades (IPH), University of Zaragoza, C/Pedro Cerbuna 12, 50071 Zaragoza, Spain
* Correspondence: pmr@unizar.es

Abstract: The River Vero canyon (Huesca, Spain) contains an exceptional archaeological legacy with more than sixty rock shelters with cave paintings and forms part of the World Heritage 'Rock Art of the Mediterranean Basin on the Iberian Peninsula'. This study presents the results of the in situ and non-destructive multi-elemental composition analysis of the pigments used in eight of the main shelters through portable X-ray fluorescence spectroscopy (pXRF). Specifically, the cave paintings of the rock shelters of Chimiachas, Muriecho, and Arpán (Levantine Art); and Mallata, Barfaluy, Quizans, Lecina Superior, and Forau del Cocho (Schematic Art) were investigated. The red pigments, based on iron minerals, were the most abundant in all the River Vero rock shelters, with Fe contents in the 0.51–3.06% range. The iron contents of the paintings of Mallata B1 and I, Muriecho, and Forau del Cocho were higher than those of Arpán, Barfaluy, Lecina, and Chimiachas rock-shelters; and, in turn, these were higher than those of Quizans, pointing to noticeable differences in the degree of conservation. Black pigments, in the absence of manganese, were associated with bone char or carbon black. Through the phosphorus content, evidence is provided of the use of bone phosphates as a component of the paints, either as a filler or as a binder. Geological studies indicate that the detected gypsum is of external origin, probably associated with gypsum-rich atmospheric dust. The reported pXRF analysis of this large set of paintings may serve as a basis for future characterization studies involving other portable chemical analysis techniques.

Keywords: multi-elemental analysis; Schematic Art; Levantine Art; X-ray fluorescence spectroscopy; River Vero Cultural Park; rock shelter

Citation: Martín-Ramos, P.; Cuchí-Oterino, J.A.; Bea-Martínez, M. Portable X-ray Fluorescence Analysis of Levantine and Schematic Art Pigments from the River Vero Shelters (Huesca, NE Spain). *Heritage* **2023**, *6*, 3789–3800. https://doi.org/10.3390/heritage6040201

Academic Editors: Vittoria Guglielmi and Marta Manso

Received: 26 December 2022
Revised: 28 February 2023
Accepted: 19 April 2023
Published: 20 April 2023

1. Introduction

The River Vero Cultural Park is located in the Guara mountain range and neighboring areas (southern outcrops of the Central Pyrenees), in the province of Huesca (Northeastern Spain), and contains an exceptional archaeological legacy of more than 60 shelters with rock paintings, listed in [1–3], located in a few square kilometers of a wild and rugged area. In the different painted rock shelters, magnificent examples of the three classic artistic cycles of European rock art can be found: Paleolithic (40,000–10,000 B.C.E.), and two others with a post-Paleolithic chronology, viz. Levantine (8000–3000 B.C.E.) and Schematic (5000–1500 B.C.E.).

Due to the importance of this rock art nucleus, these rock art sites were added to the World Heritage List of UNESCO in 1998, as part of the 'Rock Art of the Mediterranean

Basin on the Iberian Peninsula'. In 2001, the Government of Aragon declared the River Vero Cultural Park (Decree 110/2001 of the Government of Aragon) in the application of Law 12/1997 of the Cultural Parks of Aragon, considering rock art as one of the main axes of the declaration.

Attending to the historical research on the region, the first rock art shelter was reported by P. Minvielle in 1969, pointing out a group of schematic motifs. The discovery of some other decorated sites came as a result of different survey campaigns carried out by A. Beltrán [4–6] and, above all, by V. Baldellou and his team [7–15]. After the discovery phase, the inclusion in the World Heritage List, and the declaration of the Cultural Park, the attention has been focused on the study, dissemination, documentation, and preservation of this heritage. As an example, D-laser scanning has been performed in the Arpan and Chimiachas shelters [16], and a replica of the Fuente del Trucho cave is being considered.

Pigment analyses have been carried out using destructive techniques (LA-ICPMS) in shelters of Barfaluy, Coveta de l'Engardaixo, Gallinero, Mallata, La Raja, and Cueva de Regacens [17]. However, an extensive analysis of a large set of paintings of the River Vero Cultural Park was lacking. In the present work, this research gap has been addressed using a non-destructive technique of in situ analysis: portable X-ray fluorescence spectroscopy (pXRF). During the last decade, this technique has been widely used as a method to identify pigment composition in rock art [18–22], given that its state of technological development is presently mature and robust calibration procedures are readily accomplished and widely available [23]. Despite the limitations of this technique, described in [24,25], they may be partly overcome by applying laboratory QA/QC procedures to its use. Moreover, pXRF offers advantages in comparison to other in-field portable chemical analyzers such as those based on laser-induced breakdown spectroscopy (LIBS) for the detection of elements with high ionization potential (e.g., S, P, F, Cl, and Br) and does not require a set of closely matrix-matched standards for quantitative analysis [23].

The study presented herein aimed to elucidate the chemical elements present in the post-Paleolithic paintings of the River Vero basin, investigate the presence of contaminants, and establish correlations with the degree of conservation of the paintings.

2. Materials and Methods

2.1. Studied Area and Rock Shelters

The location of the River Vero area on a map of the Iberian Peninsula and the position of the shelters studied herein are shown in Figure 1. All the shelters, except for Forau del Cocho, are located in an area of less than 20 km^2.

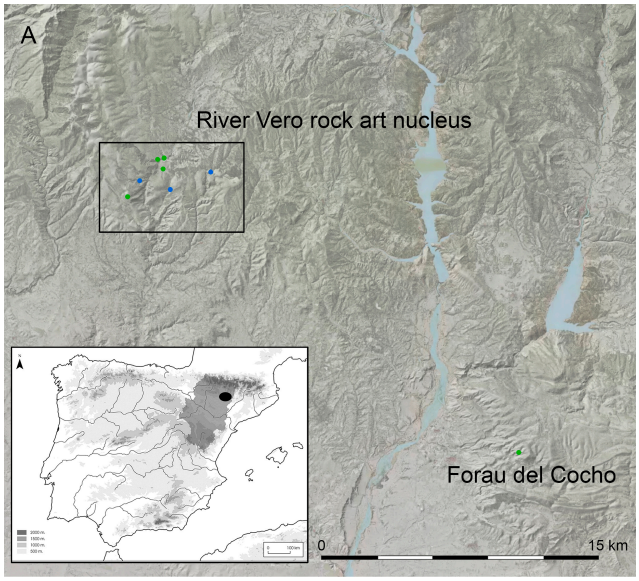

Figure 1. *Cont.*

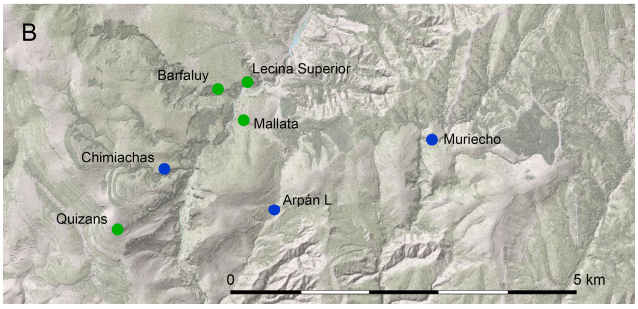

Figure 1. Location of the rock shelters in the River Vero canyon (Huesca, Northeastern Spain). Map (**B**) zooms in on the area enclosed in a box in map (**A**). Levantine Art sites are marked in blue, while Schematic Art shelters are marked in green color.

The eight painted rock shelters were selected based on the style of the paintings, number of motifs, representativeness, chrono-cultural affiliation, and degree of conservation. Levantine Art shelters of Chimiachas, Muriecho, and Arpán, together with Schematic Art shelters of Mallata, Barfaluy, Quizans, Lecina Superior, and Forau del Cocho were investigated. The latter, 27 km far from the rest as the crow flies, was included because of the relatively high intensity of its red coloration, which led some experts to suggest the presence of cinnabar as a pigment.

2.2. Geological Setting

All the shelters studied in the present work are open in limestones of the Guara formation of the Lutetian age (middle Eocene). The Guara Fm consists of a ramp of shallow marine carbonates, rich in foraminifera fossils. Additional information can be found at [26,27].

In the area of the River Vero, the Guara formation reaches thicknesses of several hundred meters, in decametric order. Due to their origin, they are bioclastic limestones. There are several studies on the petrography of the limestones of the Guara Fm. Petrographic information on the limestone near some of the studied shelters has been reported in [28]. Petrology shows a grainstone–packstone texture type, following the classical Dunhan classification. Calcite is practically the unique mineral in X-ray powder diffractograms in samples from Arpan, Mallata I, and Lecina; no gypsum was found.

The landscape is very rugged, with deep karst canyons surrounded by cliffs where there are numerous shelters, resulting from differential erosion, where the paintings are found [29].

2.3. Studied Paintings Description

The area of the River Vero is well known for its Paleolithic and post-Paleolithic (Levantine and Schematic Art) cave paintings.

This area is located in the northwestern limit of Levantine Art, which presents a strong naturalism of depictions and a clear intention in the definition of scenes [30]. In the present work, the Levantine Art paintings of Chimiachas, Muriecho, and Arpán shelters were studied. The former shelter is famous for a splendid solitary figure of a large male deer (Figure 2).

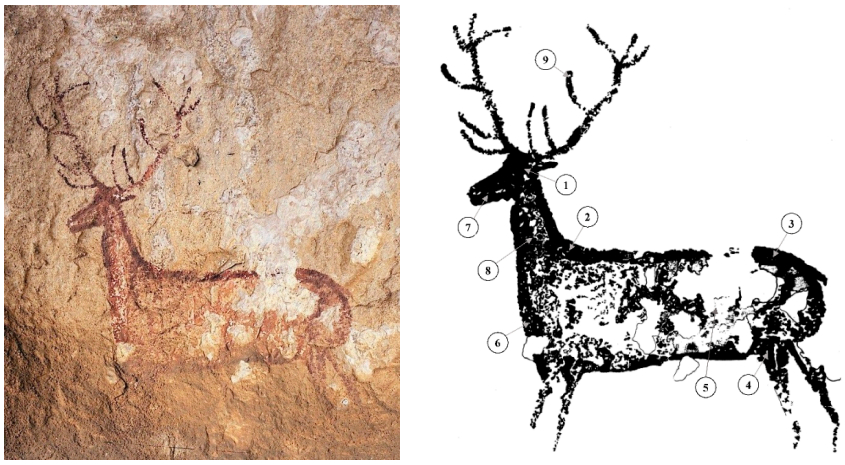

Figure 2. Chimiachas deer: (**left**) photograph; (**right**) sampling points (indicated on the tracing of the painting presented in Figure 2 in [31]).

The Muriecho shelter is divided into four panels. In the first one (Figures S1–S3), there are abundant figures that are grouped in a possible interpretation of a ceremonial scene (with human figures playing music and dancing, Figure 3), all integrated into a ritual scene of hunting a deer [32]. In panel 2, there are two anthropomorphs. In panel 3, there are unidentifiable remains. In the last one, a badly preserved deer. The hunting scene is known for its dark red paintings, with a tendency toward chestnut color.

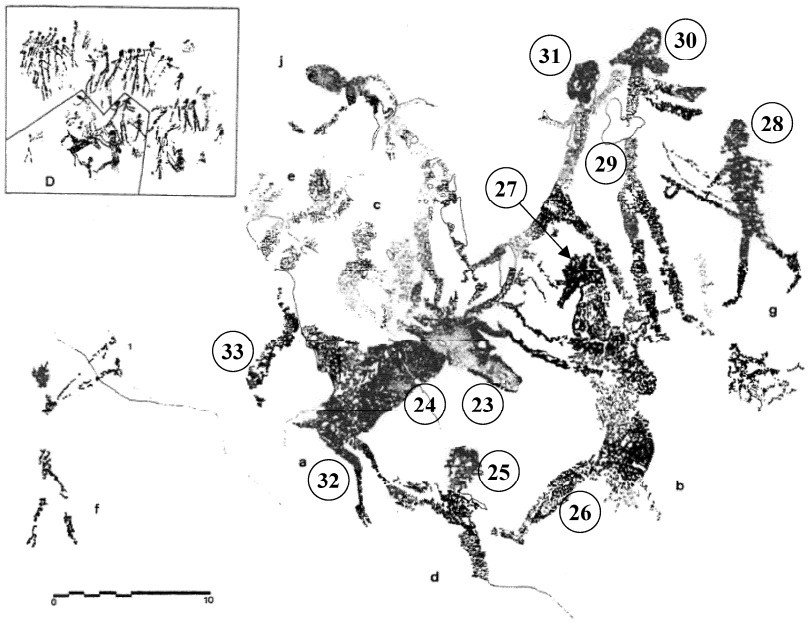

Figure 3. Section D in sector 1 of Muriecho shelter (based on the tracing of the painting presented in Figure 13 in Baldellou et al. [8]). Numbers indicate sampling points.

Concerning the Arpan shelter, it is also divided into four sectors. Sector one (Figure S4), together with unidentifiable remains, presents some animals, an archer, and, possibly, a climber. Sector two shows only smudges and informal traces. Sector three (Figures S5–S7) presents two deer, one almost complete, as well as an archer, and a possible faded human figure. Sector 4 (Figure S8) is not Levantine and presents rough figures of an archer and a deer.

With regard to Schematic Art, it is a basic and simplified style of drawing, composed of abstract and figurative motifs, such as those of the shelters of Mallata, Barfaluy, Quizans,

Lecina Superior, and Forau del Cocho. It is attributed to a wide chronology, from the ancient Neolithic to the age of metals [33].

Mallata I, B1 and C shelters hang over the Mallata cliff, where some other shelters have been recently discovered [34]. In Mallata I (Figures S9–S14), there are several anthropomorphs, one of a relatively large size, three scenes where humans tie animals by the snout, and several geometric figures, including two crosses inscribed in circles. Mallata B1 shows a number of paintings organized in three panels: panel 1 shows several anthropomorphs, two of which hold a deer using a rope (Figure S15); panel 2 consists of geometric figures (Figure S16); and in panel 3, there are several ramiforms (Figure S17).

Under the collective name of Barfaluy there are five differentiated shelters (I to V), the first three being the most important, where several sectors have been defined in each one. Figure 4 shows the most representative figures. In Barfaluy I, the first sector (Figure S18) is formed by several quadrupeds as well as humans with marked feet and hands. In the center, two human figures are flanking a third one lying down. All are fine-line motifs, red in color, and well preserved. In sector two (Figure S19), a very faded motif in the form of an occulted idol has been identified, unique in the River Vero Cultural Park. In sector three (Figures S20–S23), an enigmatic figure formed by four superimposed zigzags can be observed. In sector four, there is a single horizontal fingering. In Barfaluy II, in sector 1 (Figure S24), there are two anthropomorphs, one possibly a rider. In sector two, there are diffuse stains. In sector three, there are abstract figures, including two cross-like signs as well as an anthropomorph and a deer motif. Sector 1 of Barfaluy III (Figures S25 and S26), with black paintings, shows a quadruped and a possible anthropomorph. In sector two, there are a deer and a herd of goats/ibex. There is another herd of goats/ibex in sector 3.

Figure 4. Most representative schematic figurative motifs painted in Barfaluy I (quadrupedal), Barfaluy II (anthropomorphs and spring), and Barfaluy III (anthropomorph).

In relation to Quizans, it is worth noting that there are two shelters. In Quizans I (Figures S27 and S28), there is a deer, a small goat/ibex, digitations, and traces. In Quizans II, there is a large anthropomorph, ca. 0.5 m long.

Lecina Superior shelter (Figures S29–S33) exhibits several anthropomorphs and quadrupeds, bars, digitations, and a pectiniform sign, as well as bovids and a semi-naturalistic canid.

As for the Forau del Cocho shelter (Figures S34–S39), located in a different spatial context (in the Eastern area of the province), there are abstract signs (viz. digitations, bars, and circular strokes), as well as a semi-naturalistic cervid and two orange deer. The strong reddish color of Forau del Cocho's paintings has attracted the attention of scholars, and the presence of cinnabar has been suggested.

2.4. In Situ Measurements

Measurements were conducted from June 2020 to June 2021 with the permission of the cultural authorities of the Government of Aragón and the invaluable cooperation of the Vero Cultural Park. In situ determinations have sought to comply with the recommendations on research protocols of UNESCO-ICOMOS (International Council of Monuments and Sites), ratified at the ICOMOS 14th General Assembly (Zimbabwe, 2003), as opposed

to the traditional approach based on obtaining micro-samples and their examination in laboratories using destructive techniques [35].

The in situ, non-destructive characterization of the wall pigments was carried out with a portable X-ray fluorescence spectrometer model NITON XL3t GOLDD+ (ThermoFisher Scientific; Waltham, MA, USA), equipped with a 2 W miniaturized air-cooled X-ray tube (thin Ag anode in transmission geometry; 6−50 kV/200 μA max.) and a silicon geometrically optimized wide area drift detector (30 mm^2, 178 eV@MnKα). The range of elements to be determined includes those between Mg and U. Measurement conditions: Mining mode; light range (30 s): 8 kV, no filter; low range (30 s): 20 kV 1 Cu mil filter; main range (30 s): 38 kV, 4 Al + 1 Ti + 4 Fe mil filter; high range (30 s): 50 kV, 3 Mo + 4 Fe mil filter. Certified reference materials were used as internal standards for the dataset to monitor instrument stability. NDT™ PC software v.8.5.1 was used for spectra processing.

Analyzed points were selected according to the figures represented on each shelter, and are numbered on the tracings of the paintings presented in the supporting information (except for the points analyzed in Forau del Cocho, indicated on photographs). Several points were analyzed in large figures (e.g., in the deer motif in Chimiachas, Figure 2), while the areas with the highest color intensity were analyzed in smaller ones. In the case of human motifs, they tended to correspond to the head. In addition, measurements were also taken on the (unpainted) limestone of the shelters for comparison purposes. All measurements were conducted in triplicate, and all values presented in the results section are average values (n = 3).

2.5. Statistical Analysis

A principal component analysis (PCA) with Kaiser normalization was performed as an exploratory tool to reduce the number of variables and determine whether it was possible to divide the paintings of the eight rock shelters into groups based on their pigment/bedrock lithological characteristics. Statistical analyses were conducted in IBM SPSS software v.25 (IBM, Armonk, NY, USA).

3. Results and Discussion

3.1. Multi-Elemental Analysis

From the raw data, only the most important elements were selected, followed by normalization to 100%. Only the results of Chimiachas (Figure 2, Tables 1 and 2) and Section D of sector 1 from Muriecho (Figure 3 and Table 3) are presented in the main text. The rest are shown in the Supplementary Material (Tables S1–S11).

Table 1. Chemical composition of the deer painting from Chimiachas shelter (expressed in percentages) determined by pXRF. Sampling points are indicated on the tracing of the painting in Figure 2.

Ref. Point	Bal *	Fe	Ti	Ca	Al	Si	P	S	Cl	K
1	57.32	0.83	-	29.23	0.30	1.30	0.12	10.64	0.10	0.10
2	55.26	2.05	0.03	27.78	0.57	2.02	-	11.88	0.12	0.19
3	56.52	0.72	0.05	28.17	0.47	1.98	0.08	11.70	0.08	0.17
4	56.81	1.03	0.07	25.94	0.85	3.61	0.12	11.09	0.11	0.34
5	54.94	0.71	0.09	27.51	0.75	3.93	0.08	10.39	0.11	0.35
6	51.47	0.80	0.06	26.35	1.21	3.32	0.16	16.17	0.13	0.30
7	52.75	0.81	0.05	30.31	0.52	2.11	-	13.09	0.11	0.21
8	49.06	0.59	0.03	33.79	0.79	2.39	0.22	12.75	0.14	0.18
9	58.05	0.67	0.04	33.95	0.35	1.43	0.49	4.68	0.19	0.09
Mean value	54.69	0.91	0.05	29.23	0.64	2.46	0.18	11.38	0.12	0.21

* Bal (balance), i.e., the difference to 100% of the sum of all measured elements, includes elements with atomic number $Z \leq 11$, mainly C, N, O, F, and Na.

Table 2. Chemical composition of the substrate rock of the Chimiachas shelter (expressed in %) determined by pXRF.

Ref. Point	Bal	Fe	Ti	Ca	Al	Si	P	S	Cl	K
C1	49.01	0.04	-	36.27	-	0.82	0.25	13.27	0.09	0.04
C2	55.20	0.09	0.03	27.69	0.54	2.63	0.06	12.52	0.13	0.09
C3	46.34	0.72	0.14	27.29	2.61	7.82	0.56	13.52	0.19	0.71

C1, white spalling; C2, natural orange area; C3, dirty area at foot height.

Table 3. Chemical composition of selected paintings in section D of sector 1 of Muriecho shelter (expressed in %) determined by pXRF. Sampling points are indicated on the tracing of the painting in Figure 3.

Ref. Point	Bal *	Fe	Ti	Ca	Al	Si	P	S	Cl	K
23	51.04	1.79	0.08	30.09	1.79	4.33	1.62	8.55	0.12	0.46
24	51.39	5.25	0.09	25.50	1.60	4.21	1.15	9.88	0.10	0.59
25	48.69	3.01	0.10	26.19	1.63	4.12	0.76	13.84	0.11	0.63
26	51.37	1.78	0.10	27.84	1.99	4.79	0.84	10.41	0.15	0.63
27	56.67	2.18	0.08	25.98	1.34	3.83	1.24	7.97	0.07	0.50
28	44.65	2.07	0.07	26.56	1.53	3.44	0.61	20.43	0.05	0.46
29	44.36	1.89	0.07	26.30	1.49	3.34	0.64	21.33	0.06	0.42
30	45.65	2.47	0.07	24.92	1.93	3.99	0.47	19.88	0.06	0.48
31	51.67	1.92	0.10	25.09	1.12	3.13	0.72	15.03	0.06	0.44
32	49.49	3.80	0.10	25.09	2.11	4.86	0.66	12.93	0.07	0.68
33	47.57	0.90	0.10	25.17	1.88	4.18	0.41	19.05	0.05	0.60
Mean value	49.32	2.46	0.09	26.25	1.67	4.02	0.83	14.48	0.08	0.53

* Bal (balance), i.e., the difference to 100% of the sum of all measured elements, includes elements with atomic number $Z \leq 11$, mainly C, N, O, F, and Na.

Table 4 shows the mean values of the measurements conducted in the different rock shelters.

Table 4. Average values of the chemical composition of the parietal paintings of the River Vero shelters determined by pXRF.

Shelter	Bal *	Fe	Ti	Ca	Al	Si	P	S	Cl	K
Chimiachas	54.69	0.91	0.05	29.23	0.64	2.46	0.18	11.38	0.12	0.21
Muriecho	49.68	2.85	0.08	26.55	1.36	3.38	0.56	14.73	0.08	0.47
Arpán	52.89	2.17	0.06	28.85	1.06	3.61	0.61	10.26	0.12	0.35
Barfaluy	56.11	1.55	0.08	31.56	0.83	2.54	0.21	6.61	0.10	0.27
Lecina Superior	55.98	1.21	0.06	30.06	0.95	3.19	0.48	7.07	0.09	0.29
Forau del Cocho	51.48	2.72	0.05	28.80	0.88	2.66	0.34	12.44	0.15	0.25
Mallata	54.77	3.06	0.06	29.81	0.89	3.01	0.36	7.46	0.15	0.29
Quizans	51.51	0.74	0.09	28.53	1.09	3.33	0.67	13.56	0.10	0.28

* Bal (balance), i.e., the difference to 100% of the sum of all measured elements, includes elements with atomic number $Z \leq 11$, mainly C, N, O, F, and Na.

Given the red color of most of the paintings, it is not a surprise that iron was the most important chromophore in the pigments, as in most of the prehistoric rock paintings in the Mediterranean Spanish area [19,25,36–38]. One plausible local origin of this pigment could be the iron nodules (hematite, altered to goethite or even limonite) that appear scattered in nearby Eocene marine limestones [29]. The geological origin of these accumulations is unknown. Another possibility would be the use of ochre, a mixture of iron oxides with decalcification clays. A nearby cavity is known from which this material has been extracted at different times [39].

The iron contents of the paintings of Forau del Cocho, Mallata B1 and I, and Muriecho were higher than those of Arpán, Barfaluy, Lecina, and Chimiachas. The lowest values were

observed at the Quizans shelter. If such iron content is adopted as a marker of the state of conservation (given that various physical, chemical, biological, and geological processes alter the surface of the rock and the paintings [36,37]), the best-preserved paintings would be those of Mallata and the worst-preserved would be those of Quizans. However, it cannot be ruled out that iron contents vary as a function of different techniques/pictorial recipes by different authors at different times. It is also worth noting that iron was detected in the bedrock in areas where paintings were not visible to the naked eye (albeit in much lower concentrations). Its presence may have a natural origin, although it may also be associated with disappeared paintings.

Contrary to some expectations, no mercury was found at Forau del Cocho, ruling out the use of cinnabar as a red pigment.

The titanium content in the paintings was very low, as it occurs in ferruginous nodules such as the one analyzed in [29].

Manganese was not detected in any of the studied post-Paleolithic paintings, including the black ones (for which it had been hypothesized as the most probable pigment in the literature, in line with the presence of manganese in other Levantine Art black paintings [19]). Surprisingly, it was detected in Paleolithic paintings in the nearby Fuente del Trucho cave [40].

In the absence of manganese, the black color of some paintings can be associated either with carbon black or bone char, in line with the findings of other authors (e.g., [36,41–43]) in other Levantine and Schematic Art sites of the Iberian Peninsula. In those measurements, there is a high percentage of Bal, which gathers the light elements (C, N, O, F, Na) and among which carbon is found; however, the method does not discriminate between C from charring organic materials and that from carbonate (limestone bedrock). It must be taken into account that the X-ray emission from the equipment passes through the thin and discontinuous pigment layer (whose thickness varies from 2 to 5 μm, according to Resano et al. [17]) and, therefore, also scans the underlying bedrock, a fact that has been highlighted in works such as [21] (whereas, for instance, LA-ICPMS and LIBS would allow depth-profiling). For this reason, the presence of calcium is ubiquitous in all measurements. Apart from the substrate rock, it can also be linked to coatings, either inorganic (e.g., calcium carbonate films) or of bacterial origin (such as calcium oxalate), or to atmospheric dust. Moreover, due to the historical presence of cattle dung, some caves show dense partial covers of black soot, from spontaneous fires. Evidently, the known paintings are outside these areas, but it is possible that there may be some carbonaceous particles on them that contribute to part of the carbon in the Bal percentage. Raman spectroscopy measurements would be particularly useful to gain further insight into the composition of these black paintings [44].

The presence of phosphorus is quite irregular in the paintings, as well as in the supporting rock. It is evident in the dark Muriecho paintings but not in the Barfaluy I ones. This would perhaps allow distinguishing the carbon black pigments (much more frequent in Levantine Art contexts [25]) from the bone char ones, but it is highly possible that marrow, from crushed bones, was used as a binder for the paints in some cases. Furthermore, some of the shelters have served as cattle corrals and it is possible that the animal droppings and bone remains may have partially covered the walls of the shelters.

Silica and aluminum contents can be ascribed to clays, either from the decalcification of the limestone substrate or contributed by atmospheric dust [36]. The potassium possibly has the same origin, given that the presence of illite is general in the River Ebro basin.

There is a manifest presence of sulfur in all the paintings, but it also appears in the measurements on the unpainted rock. In a first approximation, several hypotheses may be considered: sulfur may come from the substrate rock in the form of gypsum or as a sulfide, it can be part of the paint, or it may come from the outside, either as an atmospheric pollutant (such as gas, dust, smoke) or brought in by rainwater. The presence of gypsum was ruled out by X-ray powder diffraction analysis of fresh rock samples from Arpán and Chimachas shelters [28], which only showed calcite. Another possibility would be the

oxidation of pyrite present in the marine sediments that gave rise to the limestones and that, by oxidation, could yield gypsum and the accumulations of nodules of iron(III). However, the presence of pyrite is unknown in limestone quarries throughout the Pre-Pyrenees, elevated since the middle Eocene and subjected to long and intense karstification processes with infiltration of oxygen-rich atmospheric waters. The presence of sulfur in animal fats or bird egg albumin used as binders in paints is also very low. Consequently, the sulfur found on the surface of the rock must have been deposited by an external contribution. The formation of gypsum by reaction between atmospheric SO_2 and calcite from the rock has been suggested by Hernanz et al. [36], but the area under study is uninhabited and isolated, far from industrial areas. For example, the distance, as the crow flies, between the River Vero area and the Andorra thermal power plant, a known sulfur emitter due to lignite burning, is more than 130 km. Sulfur content in local vegetation is too low to assume its significant presence in smoke from forest fires or nearby campfires. Hence, atmospheric transport of gypsum, very abundant in the nearby semi-arid Ebro valley (where dust storms are common) may be regarded as the most probable origin. This gypsum would impregnate the rock surface, either by dry deposition or dissolved in rainwater.

The origin of the chlorine content is also complex to assign. Its presence seems to be exogenous to the limestone substrate of the area and may be ascribed to an atmospheric dust contribution.

Little can be said about the differences among individual paintings in each of the shelters. Practically all the measurements (except for those carried out in Chimiachas), were made on different figures. It is very possible that such figures are not contemporary and, in some cases, color changes can be appreciated by the naked eye. In addition, the possibility that some of them may have been repainted in antiquity cannot be discarded. This would need a more detailed study. As for the measurements carried out on the deer of Chimiachas, an emblematic painting of the area, the results (Table 1) were very homogenous for all elements except for iron, whose higher contents in some measurements may be due to a greater application of pigment or less alteration.

What seems clear, in view of the mean values of the average results per element of the various shelters (Table 4), is that all the studied post-Paleolithic sets of paintings have a very similar composition.

3.2. Statistical Analysis

Statistical analysis of the 225 measurements conducted on paintings (excluding bedrock measurements) yielded the correlation matrix shown in Table 5. Correlation coefficients were generally low.

Table 5. Correlation coefficients between the different elements measured in the rock paintings of several shelters of the Vero River Cultural Park.

	Fe	**Ti**	**Ca**	**Al**	**Si**	**P**	**S**	**Cl**	**K**
Fe	1	−0.178	−0.542	0.020	−0.062	0.099	0.040	0.065	0.146
Ti	−0.178	1	−0.225	0.623	0.623	0.345	−0.057	−0.144	0.650
Ca	−0.542	−0.225	1	−0.249	−0.239	−0.315	−0.427	0.076	−0.481
Al	0.020	0.623	−0.249	1	0.847	0.625	0.018	0.057	0.726
Si	−0.062	0.623	−0.239	0.847	1	0.565	−0.178	0.175	0.699
P	0.099	0.345	−0.315	0.625	0.565	1	0.025	0.058	0.517
S	0.040	−0.057	−0.427	0.018	−0.178	0.025	1	−0.308	0.047
Cl	0.065	−0.144	0.076	0.057	0.175	0.058	−0.308	1	0.049
K	0.146	0.650	−0.481	0.726	0.699	0.517	0.047	0.049	1

Iron did not correlate with the rest of the elements detected by pXRF. This absence of correlation is in agreement with the findings of Resano et al. [17], who—using LA-ICPMS on schematic style paintings found in several River Vero shelters—reported that only As, Co, Mo, Sb, Tl, and Zr showed a high correlation with Fe. The inverse correlation of iron

with calcium may be related to the coating layers (patina) developed on the paint layer, a particularly interesting topic that deserves further examination in future work. The low correlation coefficient of iron with sulfur also excludes the use of gypsum in the painting process as an extender to bulk out the pigment or as a ground for painting (i.e., as a primer).

Titanium did not correlate with iron and thus cannot be regarded as a useful trace element for the characterization of the red pictograms. On the other hand, such an absence of correlation would support the hypothesis of the iron-rich nodules as the most probable origin of the iron used in the pigments, given that Ti correlated well with the clay components (Si, Al, and K) expected in an ochre.

The moderate correlation of phosphorus with the clay elements is also interesting and an aspect that should be studied in more detail.

The fact that chlorine did not correlate with the rest of the elements, except for sulfur, further supports the aforementioned atmospheric contribution origin.

A series of principal component analyses were carried out in an attempt to find differences between the different paintings or shelters (detailed in supporting information). When all the elements were considered, a clear dominance of calcium, logically derived from the support rock, was observed (in agreement with the findings of Chanteraud et al. [21] on calcium dominance). PCA analyses did not allow for pigment discrimination among shelters (Figure S40).

4. Conclusions

Almost all of the post-Paleolithic paintings analyzed in the River Vero rock shelters have been made with iron(III) oxides (hematite), probably obtained from iron nodules scattered in the Eocene marine limestones. The presence of manganese-based pigments in dark-colored paintings and that of cinnabar in the vivid red paintings from the Furau del Cocho—hypothesized in the literature—could be ruled out. In the case of dark paintings, carbon black or bone char may be put forward as the most probable constituents. The presence of phosphorus may be related either to bone char or to the use of bone marrow or crushed bone in the paintings. Concerning contaminants, the presence of sulfur and chlorine should be primarily ascribed to atmospheric deposition. As regards the correlation between iron content and the degree of conservation of the paintings, the results are consistent with visual inspections and it may serve the authorities to select those of priority interest for such subsequent detailed studies and conservation actions, particularly necessary in the Quizans shelter.

Supplementary Materials: The following supporting information can be downloaded at: https://www.mdpi.com/article/10.3390/heritage6040201/s1, Figures S1–S39: Sampled points in the various shelters; Tables S1–S11: Chemical composition of the paintings and the bedrock of the various shelters determined by pXRF; Figure S40: F2 vs. F1 biplot, and F3 vs. F1 biplot. Reference [45] is cited in the supplementary materials.

Author Contributions: Conceptualization, J.A.C.-O.; methodology, P.M.-R.; validation, M.B.-M.; formal analysis, P.M.-R.; investigation, P.M.-R., J.A.C.-O. and M.B.-M.; resources, P.M.-R.; writing—original draft preparation, P.M.-R., J.A.C.-O. and M.B.-M.; writing—review and editing, P.M.-R. and J.A.C.-O.; visualization, P.M.-R.; supervision, J.A.C.-O.; project administration, P.M.-R.; funding acquisition, P.M.-R. All authors have read and agreed to the published version of the manuscript.

Funding: This work is funded by the BBVA Foundation as part of the Leonardo Grant to Researchers and Cultural Creators 2019 program. The BBVA Foundation is not responsible for the opinions, comments, and contents included in the project and/or the results obtained from it, which are the total and absolute responsibility of their authors.

Institutional Review Board Statement: Not applicable.

Informed Consent Statement: Not applicable.

Data Availability Statement: The data presented in this study are available on request from the corresponding author.

Acknowledgments: The authors thank the Parque Cultural del Río Vero staff for their cooperation in this study, in particular Maria Nieves Juste (Director of the River Vero Cultural Park) and Rosa Berges (rock art guide).

Conflicts of Interest: The authors declare no conflict of interest. The funders had no role in the design of the study; in the collection, analyses, or interpretation of data; in the writing of the manuscript; or in the decision to publish the results.

References

1. Utrilla Miranda, M.d.P. *El Arte Rupestre en Aragón*; Caja de Ahorros de la Inmaculada de Aragón (CAI): Zaragoza, Spain, 2000; p. 94.
2. Hameau, P.; Painaud, A. L'expression schématique en Aragon présentation et recherches récentes. *L'Anthropologie* **2004**, *108*, 617–651. [CrossRef]
3. Bea-Martínez, M.; Lanau-Hernáez, P. *Corpus del Arte Rupestre del Alto Aragón*; Instituto de Estudios Altoaragoneses, Diputación Provincial de Huesca: Huesca, Spain, 2021; p. 298.
4. Beltrán Martínez, A. Las pinturas rupestres de Colungo (Huesca): Problemas de extensión y relaciones entre el Arte paleolítico y el Arte levantino. *Caesaraugusta* **1979**, *49–50*, 81–88.
5. Beltrán Martínez, A. La conservación del Arte Rupestre. *Cuad. Prehist. Arqueol. Castellon.* **1987**, *13*, 61–82.
6. Beltrán Martínez, A. Las figuras "seminaturalistas" y los signos geométricos de los abrigos del "Forau del Cocho", en Estadilla (Huesca): Problemas en torno al arte "esquemático". *Arch. Prehist. Levant.* **1990**, *20*, 279–298.
7. Baldellou Martínez, V.; Painaud Guillaume, A.; Calvo Ciria, M.J. Dos nuevos covachos con pinturas naturalistas en el Vero (Huesca). In *Estudios en Homenaje al Dr. Antonio Beltrán Martínez*; Universidad de Zaragoza, Facultad de Filosofía y Letras: Zaragoza, Spain, 1986; pp. 115–133.
8. Baldellou, V.; Ayuso, P.; Painaud, A.; Calvo, M.J. Las pinturas rupestres de la partida de Muriecho (Colungo y Bárcabo, Huesca). *Bols. Rev. Arqueol. Inst. Estud. Altoaragoneses* **2000**, *17*, 33–86.
9. Baldellou, V.; Painaud, A.; Calvo, M.J. Las pinturas esquemáticas del Tozal de Mallata (Asque-Colungo. Huesca). *Zephyrus Rev. Prehist. Arqueol.* **1983**, *36*, 123–129.
10. Baldellou, V.; Painaud, A.; Calvo, M.J. Las pinturas esquemáticas de Quizáns y Cueva Palomera (Alquézar. Huesca). *Zephyrus Rev. Prehist. Arqueol.* **1983**, *36*, 117–122.
11. Baldellou, V.; Painaud, A.; Calvo, M.J. Las pinturas esquemáticas de Mallata B (Huesca). *Boletín Mus. Zaragoza* **1985**, *4*, 17–36.
12. Baldellou, V.; Painaud, A.; Calvo, M.J. Los covachos pintados de Lecina Superior, del Huerto Raso y de la Artica del Campo (Huesca). *Bols. Rev. Arqueol. Inst. Estud. Altoaragoneses* **1988**, *5*, 147–174.
13. Baldellou, V.; Painaud, A.; Calvo, M.J.; Ayuso, P. Las pinturas esquemáticas de la partida de Barfaluy (Lecina-Bárcabo. Huesca). *Empúries* **1986**, *48–50*, 64–83.
14. Baldellou, V.; Painaud, A.; Calvo, M.J.; Ayuso, P. Las pinturas rupestres del barranco de Arpán (Asque-Colungo, Huesca). *Bols. Rev. Arqueol. Inst. Estud. Altoaragoneses* **1993**, *10*, 31–96.
15. Painaud Guillaume, A.; Ayuso, P. El legado rupestre de Vicente Baldellou. In *Corpus del Arte Rupestre del Alto Aragón*; Bea Martínez, M., Lanau Hernáez, P., Eds.; Instituto de Estudios Altoaragoneses, Diputación Provincial de Huesca: Huesca, Spain, 2021; pp. 79–93.
16. Bea, M.; Angás, J. The conservation of Spanish Levantine Rock-Art in Aragón, Spain, Using 3-D Laser Scanning. In *Open-Air Rock-Art Conservation and Management: State of the Art and Future Perspectives*; Darvill, T., Batarda Fernandes, A., Eds.; Routledge: New York, NY, USA, 2014; pp. 179–186.
17. Resano, M.; García-Ruiz, E.; Alloza, R.; Marzo, M.P.; Vandenabeele, P.; Vanhaecke, F. Laser ablation-inductively coupled plasma mass spectrometry for the characterization of pigments in prehistoric rock art. *Anal. Chem.* **2007**, *79*, 8947–8955. [CrossRef] [PubMed]
18. Beck, L.; Rousselière, H.; Castaing, J.; Duran, A.; Lebon, M.; Moignard, B.; Plassard, F. First use of portable system coupling X-ray diffraction and X-ray fluorescence for in-situ analysis of prehistoric rock art. *Talanta* **2014**, *129*, 459–464. [CrossRef] [PubMed]
19. Roldán, C.; Murcia-Mascarós, S.; Ferrero, J.; Villaverde, V.; López, E.; Domingo, I.; Martínez, R.; Guillem, P.M. Application of field portable EDXRF spectrometry to analysis of pigments of Levantine rock art. *X-Ray Spectrom.* **2010**, *39*, 243–250. [CrossRef]
20. Sepúlveda, M.; Gutiérrez, S.; Cárcamo, J.; Oyaneder, A.; Valenzuela, D.; Montt, I.; Santoro, C.M. In situ X-ray fluorescence analysis of rock art paintings along the coast and valleys of the Atacama Desert, Northern Chile. *J. Chil. Chem. Soc.* **2015**, *60*, 2822–2826. [CrossRef]
21. Chanteraud, C.; Chalmin, É.; Lebon, M.; Salomon, H.; Jacq, K.; Noûs, C.; Delannoy, J.-J.; Monney, J. Contribution and limits of portable X-ray fluorescence for studying Palaeolithic rock art: A case study at the Points cave (Aiguèze, Gard, France). *J. Archaeol. Sci. Rep.* **2021**, *37*, 102898. [CrossRef]
22. Trosseau, A.; Maigret, A.; Coquinot, Y.; Reiche, I. In situ XRF study of black colouring matter of the Palaeolithic figures in the Font-de-Gaume cave. *J. Anal. At. Spectrom.* **2021**, *36*, 2449–2459. [CrossRef]
23. Lemière, B.; Harmon, R.S. XRF and LIBS for field geology. In *Portable Spectroscopy and Spectrometry*; Crocombe, R., Leary, P., Kammrath, B., Eds.; Wiley: Hoboken, NJ, USA, 2021; pp. 455–497. [CrossRef]

24. Zerboni, A.; Dayet, L.; d'Errico, F.; García Diez, M.; Zilhão, J. Critical evaluation of *in situ* analyses for the characterisation of red pigments in rock paintings: A case study from El Castillo, Spain. *PLoS ONE* **2022**, *17*, e0262143. [CrossRef]
25. Domingo Sanz, I.; Vendrell, M.; Chieli, A. A critical assessment of the potential and limitations of physicochemical analysis to advance knowledge on Levantine rock art. *Quat. Int.* **2021**, *572*, 24–40. [CrossRef]
26. Silva-Casal, R.; Aurell, M.; Payros, A.; Pueyo, E.L.; Serra-Kiel, J. Carbonate ramp drowning caused by flexural subsidence: The South Pyrenean middle Eocene foreland basin. *Sediment. Geol.* **2019**, *393–394*, 105538. [CrossRef]
27. Silva-Casal, R.; Serra-Kiel, J.; Rodriguez-Pintó, A.; Pueyo, E.L.; Aurell, M.; Payros, A. Systematics of Lutetian Larger Foraminifera and magneto-biostratigraphy from the South Pyrenean Basin (Sierras Exteriores, Spain). *Geol. Acta* **2021**, *19*, 0015. [CrossRef]
28. Geoartec Technical Solutions S.L. *Caracterización Petrológica e Hídrica del Soporte de las Prepresentaciones Pictóricas Rupestres de los Abrigos de LECINA Superior, Arpán y Mallata I (Huesca) [Unpublished Technical Report]*; Geoartec Technical Solutions S.L.: Zaragoza, Spain, 2014; p. 14.
29. Cuchí Oterino, J.A.; Martín Ramos, P.; Salamero, E. El marco geológico del Prepirineo. In *Corpus del Arte Rupestre del Alto Aragón*; Bea Martínez, M., Lanau Hernáez, P., Eds.; Instituto de Estudios Altoaragoneses, Diputación Provincial de Huesca: Huesca, Spain, 2021; pp. 19–28.
30. Bea Martínez, M.; Calvo Ciria, M.J. Arte levantino. In *Corpus del Arte Rupestre del Alto Aragón*; Bea Martínez, M., Lanau Hernáez, P., Eds.; Instituto de Estudios Altoaragoneses, Diputación Provincial de Huesca: Huesca, Spain, 2021; pp. 135–158.
31. Viñas Vallverdú, R.; Saucedo Sánchez de Tagle, E.R. Los cérvidos en el arte rupestre postpaleolítico. *Quad. Prehistòria Arqueol. Castelló* **2000**, *21*, 53–68.
32. Utrilla, P.; Martínez-Bea, M. La captura del ciervo vivo en el arte prehistórico. *Munibe Antropol.-Arkeol.* **2005**, *57*, 161–178.
33. Lanau Hernáez, P.; Harneau, P. Arte esquemático. In *Corpus del Arte Rupestre del Alto Aragón*; Bea Martínez, M., Lanau Hernáez, P., Eds.; Instituto de Estudios Altoaragoneses, Diputación Provincial de Huesca: Huesca, Spain, 2021; pp. 159–176.
34. Lanau, P.; Gisbert, M.; Bea, M.; Puyo, A. Prospecciones arqueológicas y nuevos hallazgos de conjuntos rupestres en el término de Colungo (Huesca). In Proceedings of the IV Congreso de Arqueología y Patrimonio Aragonés, Zaragoza, Spain, 9–10 December 2021; pp. 52–58.
35. Rogerio Candelera, M.A.; Vanhaecke, F.; Resano, M.; Marzo, P.; Porca, E.; Alloza Izquierdo, R.; Saiz Jiménez, C. Combinación de análisis de imagen y técnicas analíticas para la distinción de diferentes fases en un panel rupestre (La Coquinera II, Obón, Teruel). In *El Arte Rupestre del Arco Mediterráneo de la Península Ibérica: 10 años en la Lista del Patrimonio Mundial de la UNESCO*; López Mira, J.A., Martínez Valle, R., Matamoros de Villa, C., Eds.; Generalitat Valenciana: Valencia, Spain, 2009; pp. 327–334.
36. Hernanz, A.; Ruiz-López, J.F.; Madariaga, J.M.; Gavrilenko, E.; Maguregui, M.; Fdez-Ortiz de Vallejuelo, S.; Martínez-Arkarazo, I.; Alloza-Izquierdo, R.; Baldellou-Martínez, V.; Viñas-Vallverdú, R.; et al. Spectroscopic characterisation of crusts interstratified with prehistoric paintings preserved in open-air rock art shelters. *J. Raman Spectrosc.* **2014**, *45*, 1236–1243. [CrossRef]
37. Aramendia, J.; de Vallejuelo, S.F.-O.; Maguregui, M.; Martinez-Arkarazo, I.; Giakoumaki, A.; Martí, A.P.; Madariaga, J.M.; Ruiz, J.F. Long-term in situ non-invasive spectroscopic monitoring of weathering processes in open-air prehistoric rock art sites. *Anal. Bioanal. Chem.* **2020**, *412*, 8155–8166. [CrossRef] [PubMed]
38. Zerboni, A.; Chieli, A.; Vendrell, M.; Roldán, C.; Giráldez, P.; Domingo, I. Characterizing paint technologies and recipes in Levantine and Schematic rock art: El Carche site as a case study (Jalance, Spain). *PLoS ONE* **2022**, *17*, e0271276. [CrossRef]
39. Villarroel Salcedo, J.L.; Cuchí Oterino, J.A. La cavidad conocida como Sotarraña, en Betorz (Huesca). *Lucas Mallada Rev. Cienc.* **2013**, *15*, 191–201.
40. Cuchí Oterino, J.A.; Martin-Ramos, P. Sobre la composición elemental de los pigmentos de las pinturas rupestres de los abrigos del río Vero (Huesca). In Proceedings of the IV Congreso de Arqueología y Patrimonio Aragonés, Zaragoza, Spain, 9–10 December 2021.
41. Hernanz, A.; Ruiz-López, J.F.; Gavira-Vallejo, J.M.; Martin, S.; Gavrilenko, E. Raman microscopy of prehistoric rock paintings from the Hoz de Vicente, Minglanilla, Cuenca, Spain. *J. Raman Spectrosc.* **2010**, *41*, 1394–1399. [CrossRef]
42. López-Montalvo, E.; Villaverde, V.; Roldán, C.; Murcia, S.; Badal, E. An approximation to the study of black pigments in Cova Remigia (Castellón, Spain). Technical and cultural assessments of the use of carbon-based black pigments in Spanish Levantine Rock Art. *J. Archaeol. Sci.* **2014**, *52*, 535–545. [CrossRef]
43. Petraglia, M.D.; López-Montalvo, E.; Roldán, C.; Badal, E.; Murcia-Mascarós, S.; Villaverde, V. Identification of plant cells in black pigments of prehistoric Spanish Levantine rock art by means of a multi-analytical approach. A new method for social identity materialization using chaîne opératoire. *PLoS ONE* **2017**, *12*, e0172225. [CrossRef]
44. Rousaki, A.; Vandenabeele, P. In situ Raman spectroscopy for cultural heritage studies. *J. Raman Spectrosc.* **2021**, *52*, 2178–2189. [CrossRef]
45. Painaud Guillaume, A.; Ayuso, P. Algunas reflexiones sobre una nueva figura en el abrigo de Mallata I (Asque, Colungo, Huesca). *Bols. Rev. Arqueol. Inst. Estud. Altoaragoneses* **2019**, 23–30.

Portable X-Ray Fluorescence Analysis of Levantine and Schematic Art Pigments from the River Vero Shelters (Huesca, NE Spain)

Pablo Martín-Ramos, José Antonio Cuchí-Oterino and Manuel Bea-Martínez

SUPPLEMENTARY MATERIAL

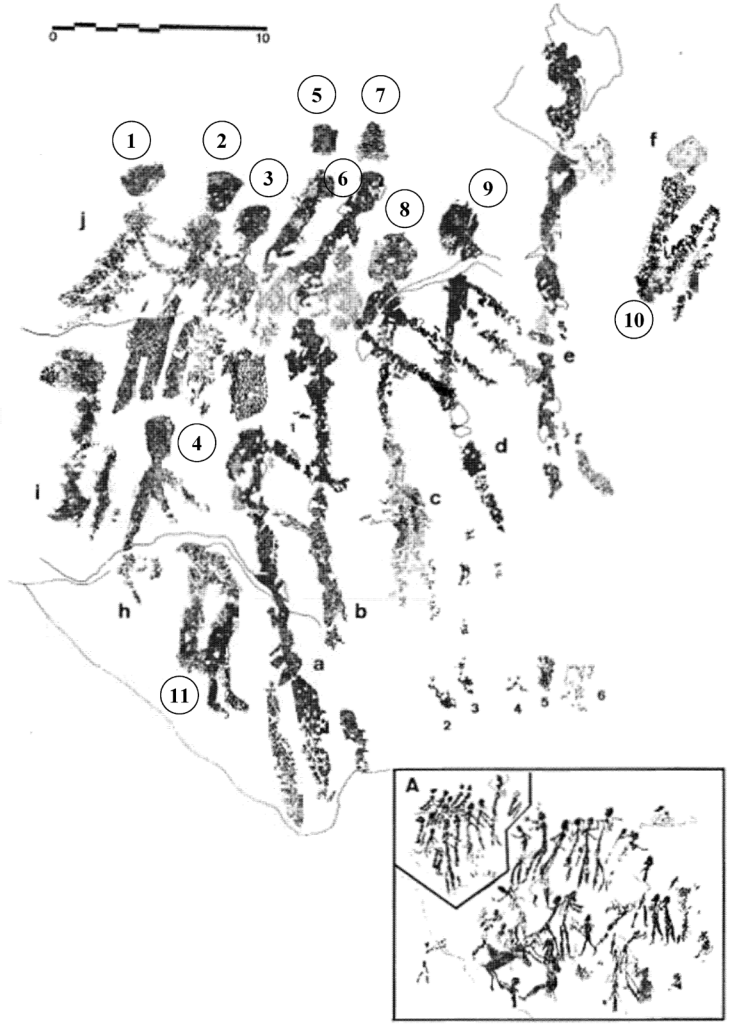

Figure S1. Sampled points in section A of sector 1 of Muriecho shelter (based on the tracing of the paintings presented in Figure 10 in [1]).

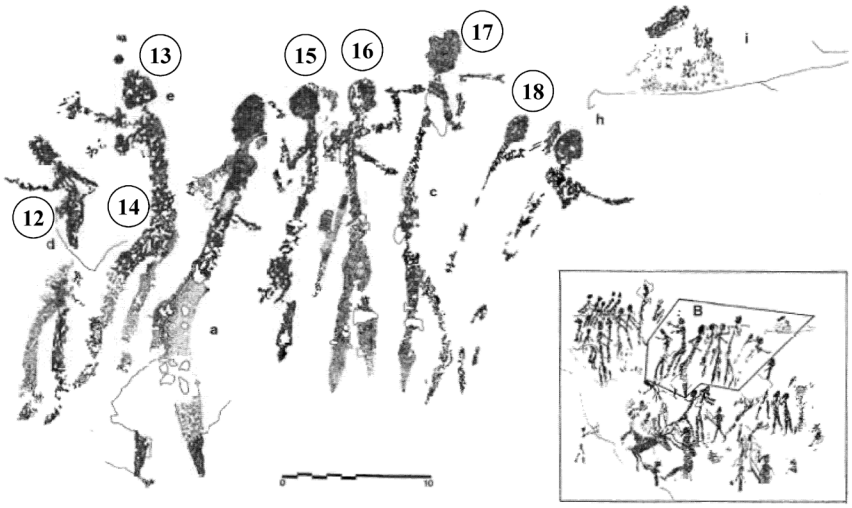

Figure S2. Sampled points in section B of sector 1 of Muriecho shelter (based on the tracing of the paintings presented in Figure 11 in [1]).

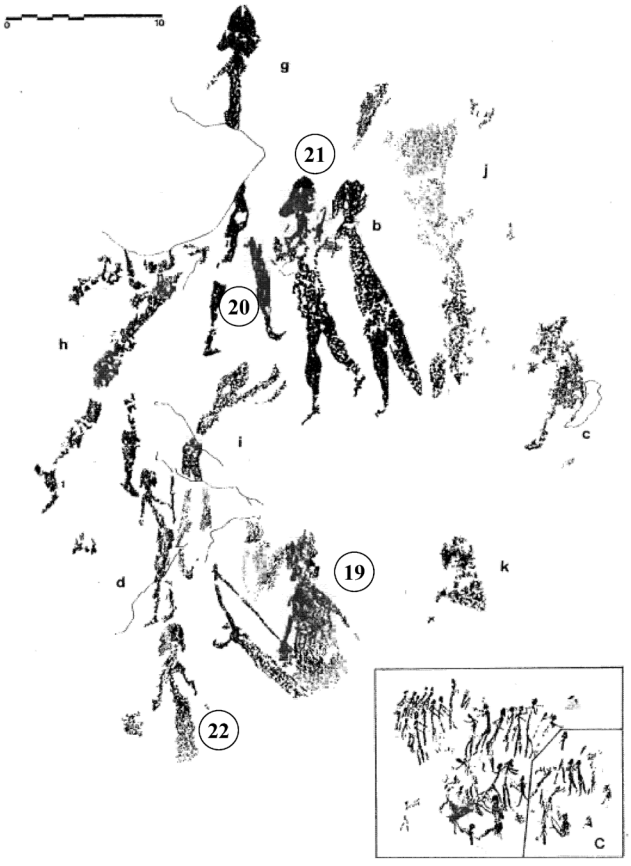

Figure S3. Sampled points in section C of sector 1 of Muriecho shelter (based on the tracing of the paintings presented in Figure 12 in [1]).

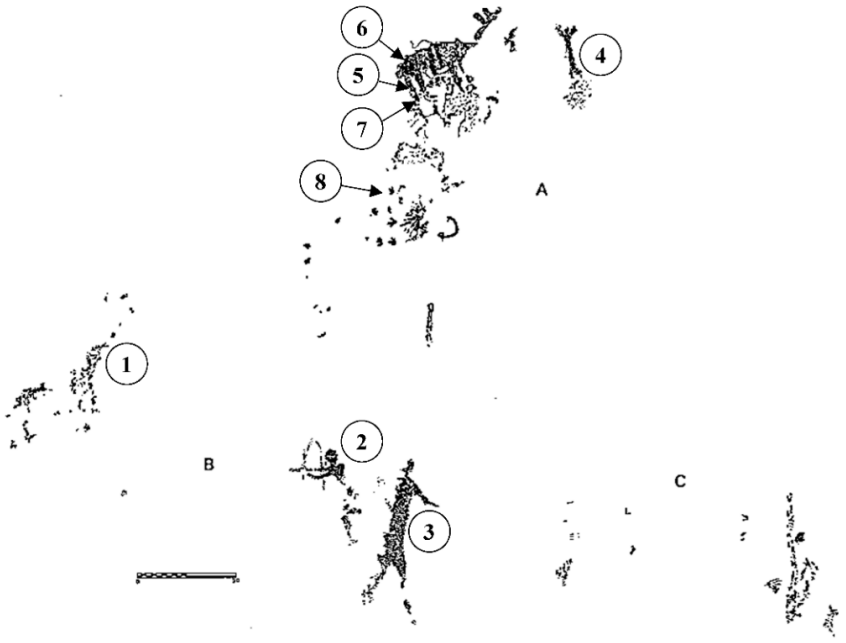

Figure S4. Sampled points in sector 1 of Arpán I shelter (based on the tracing of the paintings presented in Figure 4 in [2])

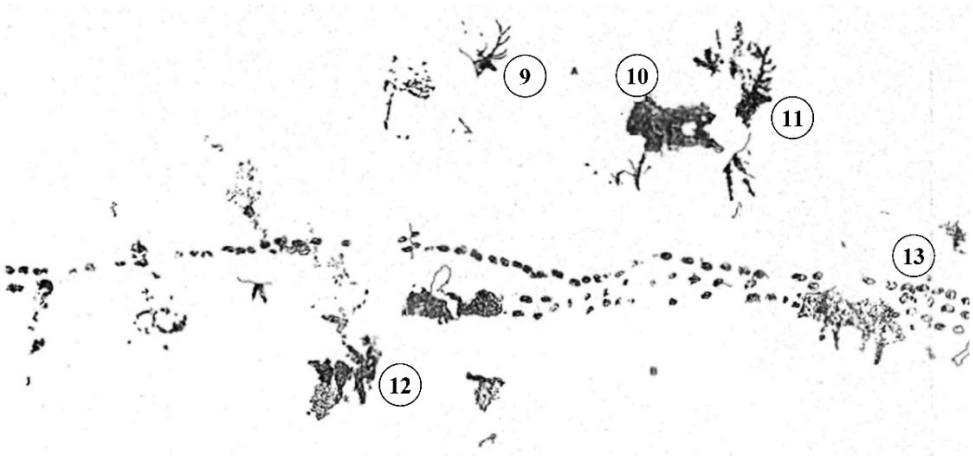

Figure S5. Sampled points in zones A and B of sector 3 of Arpán I shelter (based on the tracing of the paintings presented in Figure 10 in [2])

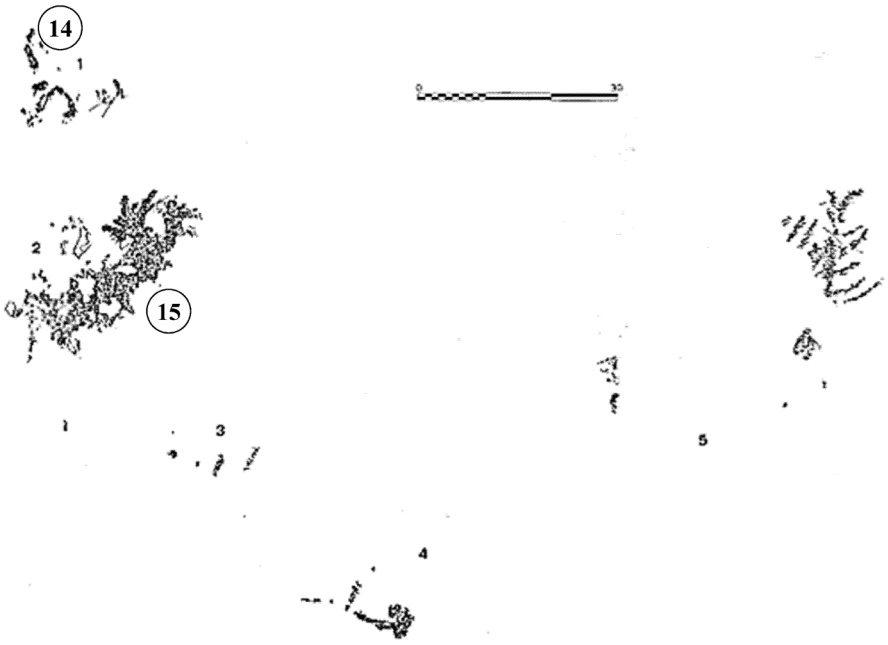

Figure S6. Sampled points in zone C of sector 3 of Arpán L shelter (based on the tracing of the paintings presented in Figure 21 in [2]).

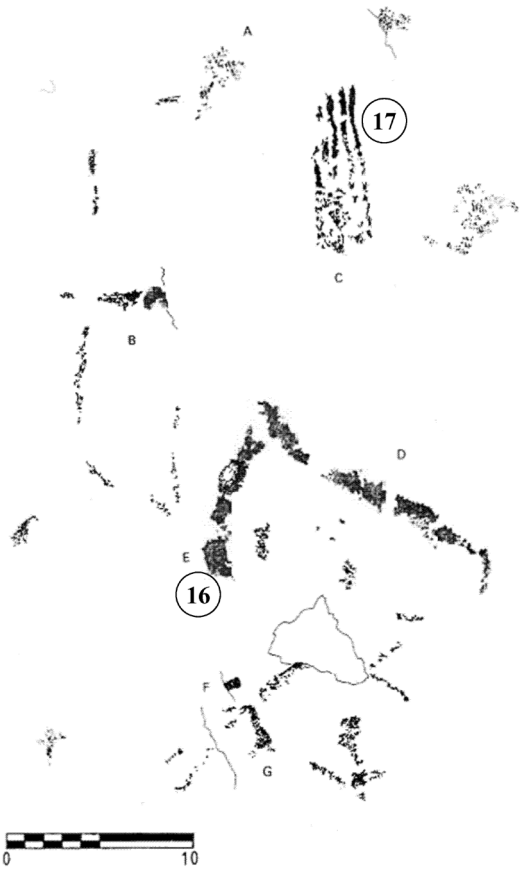

Figure S7. Sampled points in zone D of sector 3 of Arpán L shelter (based on the tracing of the paintings presented in Figure 27 in [2])

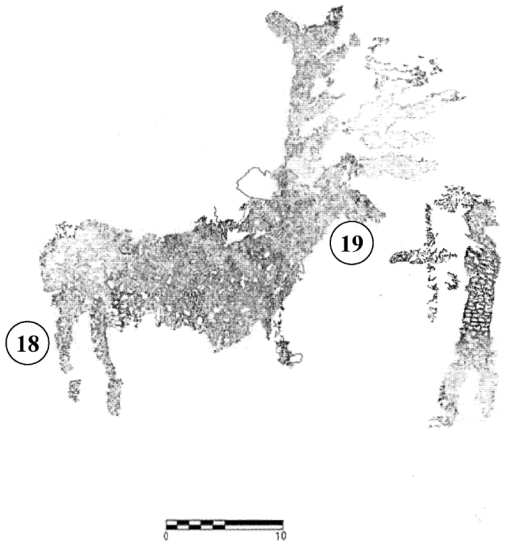

Figure S8. Sampled points in sector 4 of Arpán L shelter (based on the tracing of the paintings presented in Figure 29 in [2])

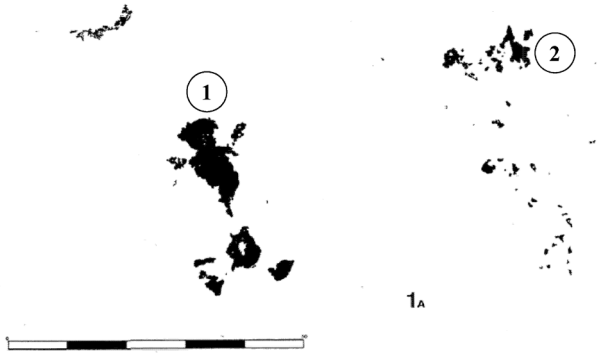

Figure S9. Sampled points in sector 1a of Mallata I shelter (based on the tracing of the paintings presented in Figure 2 in [3])

Figure S10. Sampled points in sector 1c of Mallata I shelter (based on the tracing of the paintings presented in Figure 2 in [3])

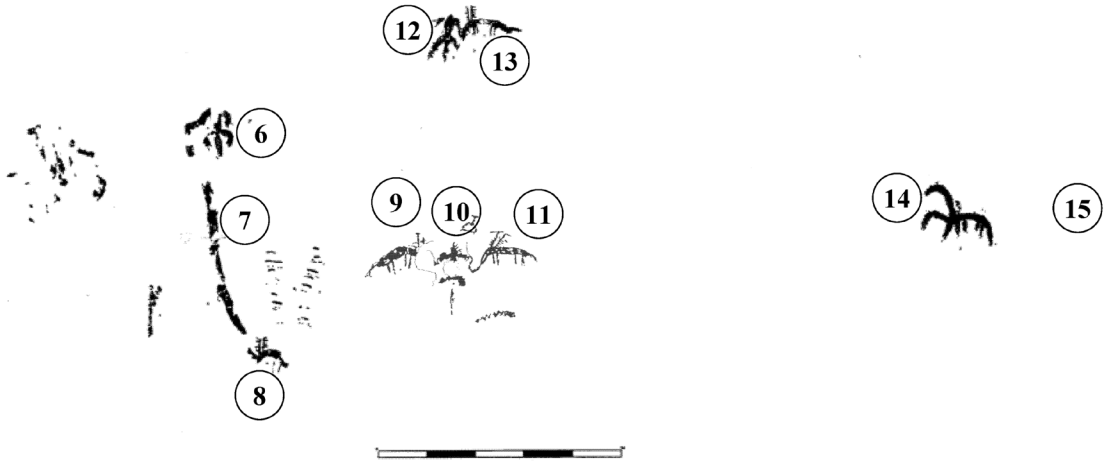

Figure S11. Sampled points in sector 2 of Mallata I shelter (based on the tracing of the paintings presented in Figure 3 in [3])

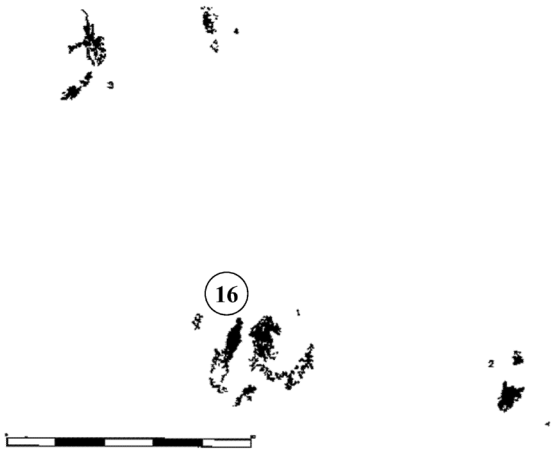

Figure S12. Sampled figure in sector 3 of Mallata I shelter.

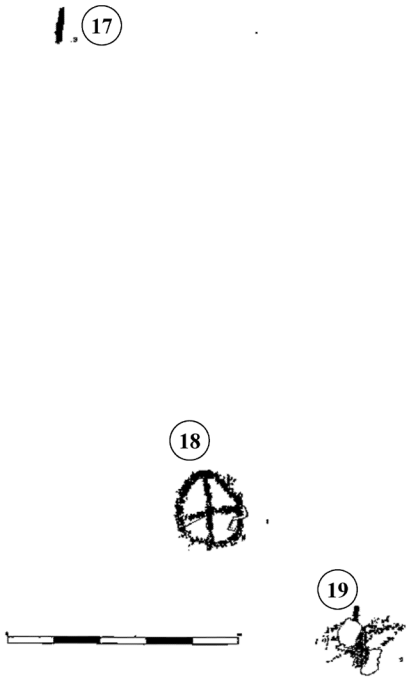

Figure S13. Sampled points in sector 4 of Mallata I shelter (based on the tracing of the paintings presented in Figure 2 in [4])

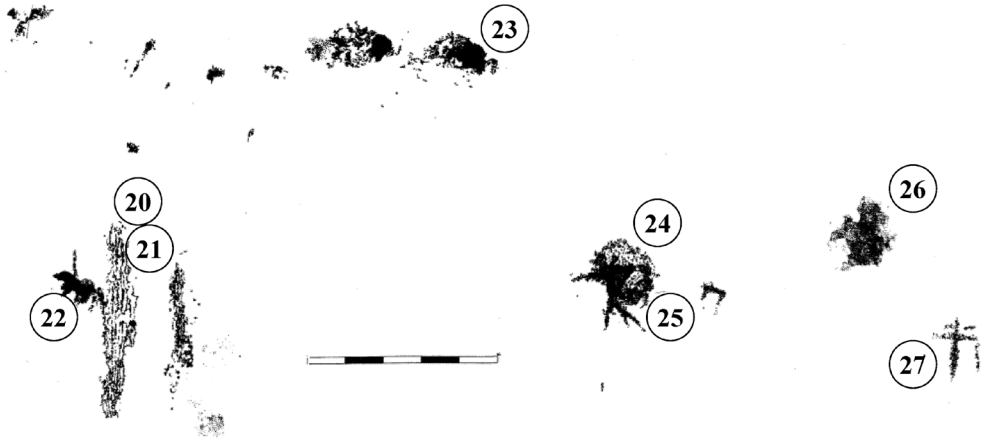

Figure S14. Sampled points in sector 5 of Mallata I shelter (based on the tracing of the paintings presented in Figure 3 in [3])

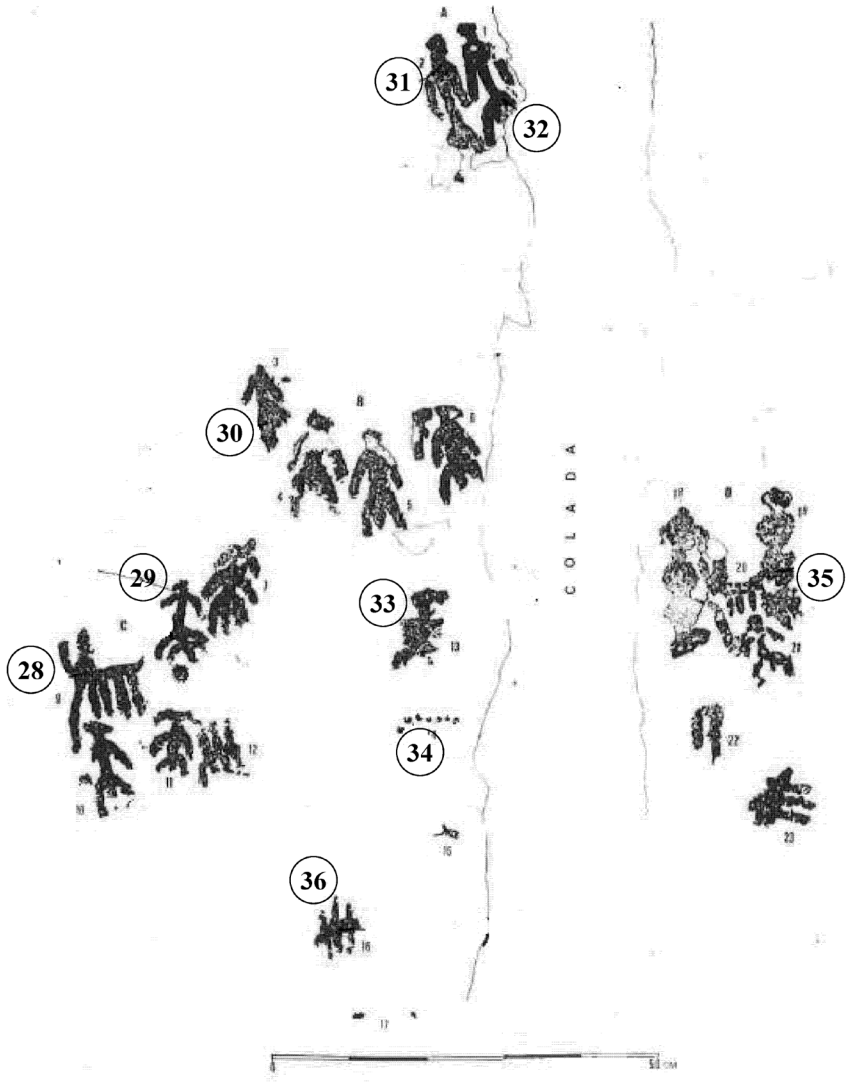

Figure S15. Sampled points in sector 1 of Mallata B1 (based on the tracing of the paintings presented in Figure 2 in [5])

Figure S16. Sampled points in sector 2 of Mallata B1 shelter (based on the tracing of the paintings presented in Figure 3 in [5])

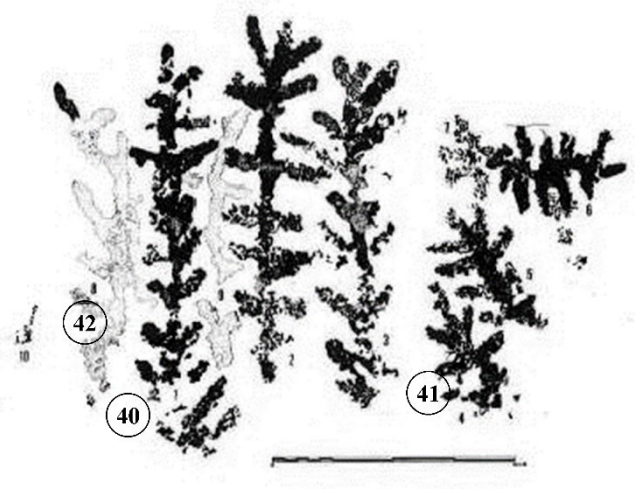

Figure S17. Sampled points in sector 3 of Mallata B1 (based on the tracing of the paintings presented in Figure 4 in [5])

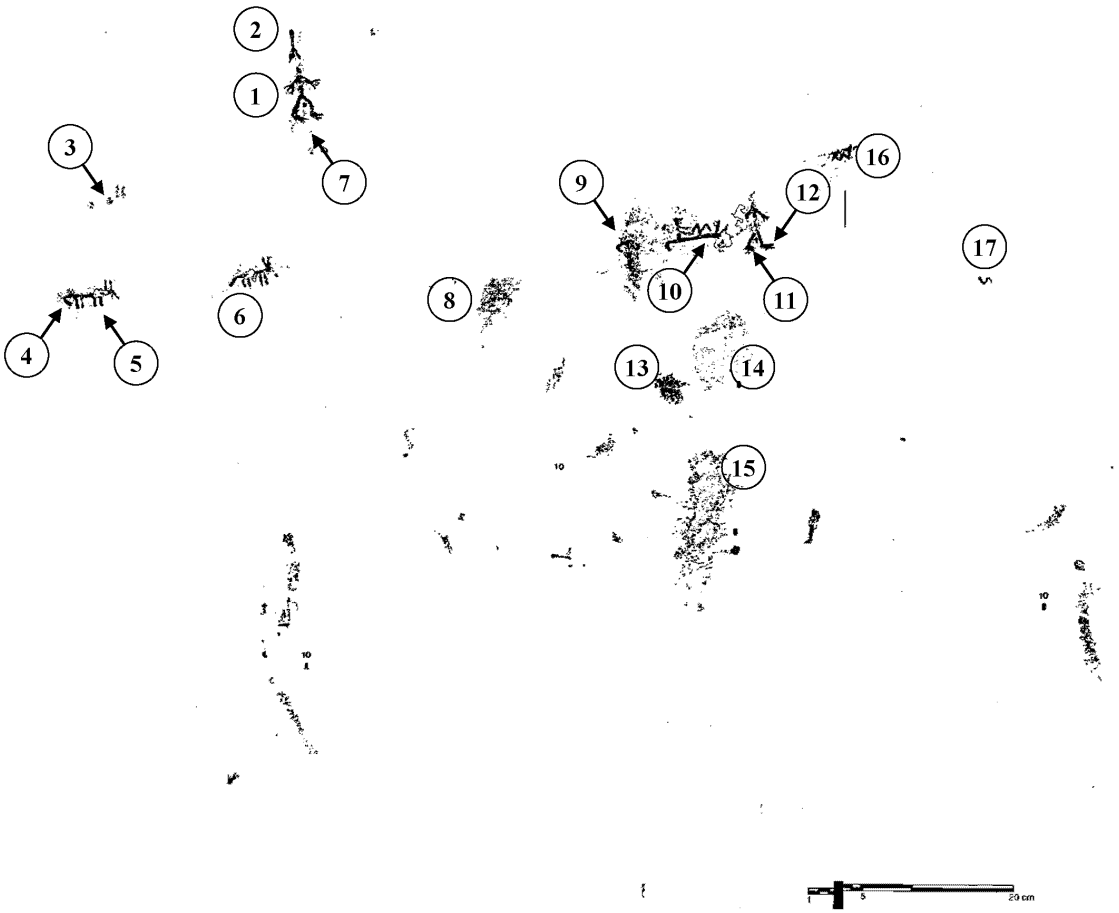

Figure S18. Sampled points in sector 1 of Barfaluy I shelter (based on the tracing of the paintings presented in Figure 5 in [6])

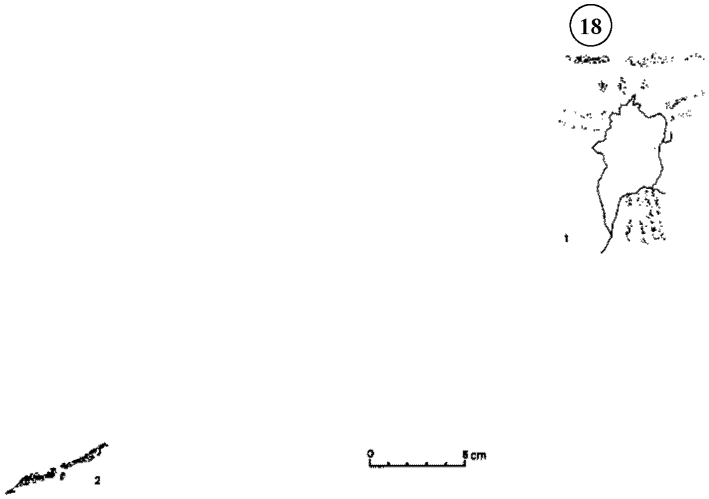

Figure S19. Sampled point in sector 2 of Barfaluy I shelter (based on the tracing of the paintings presented in Figure 6 in [6])

Figure S20. Sampled points on the figure in sector 3 of Barfaluy I shelter (based on the tracing of the painting presented in Figure 7 in [6])

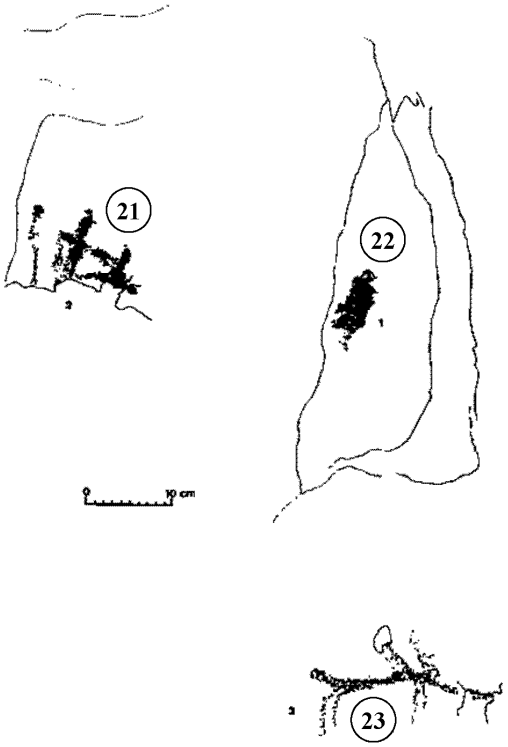

Figure S21. Sampled points on panel 3 in sector 3 of Barfaluy II shelter (based on the tracing of the paintings presented in Figure 14 in [6])

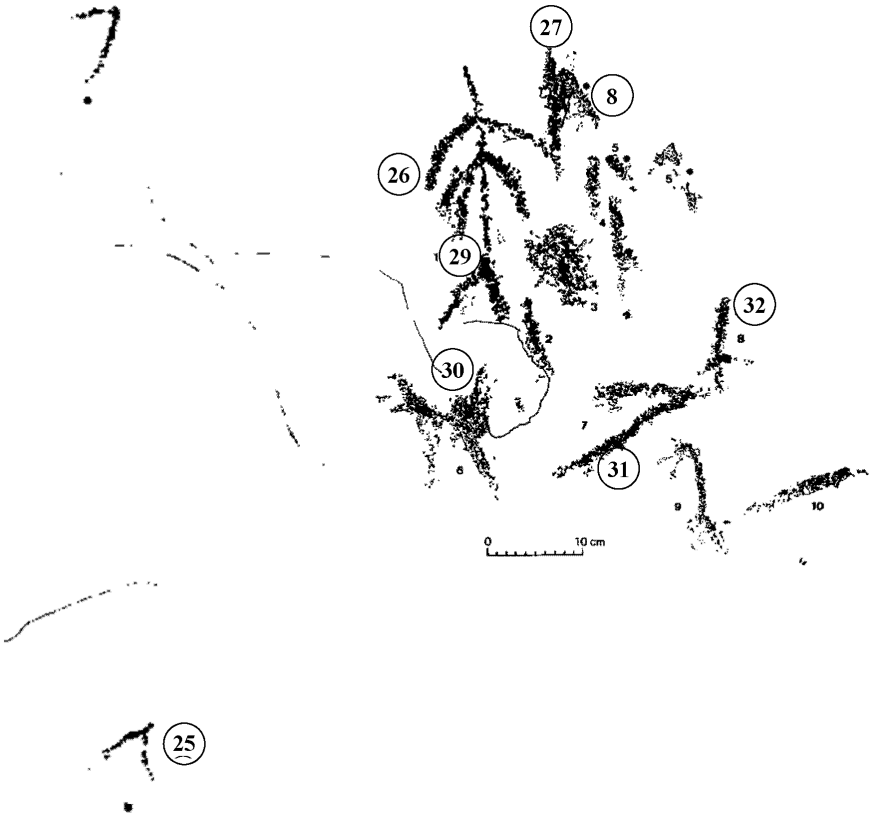

Figure S22. Sampled points on panel 2 in sector 3 of Barfaluy II shelter (based on the tracing of the paintings presented in Figures 11 and 13 in [6])

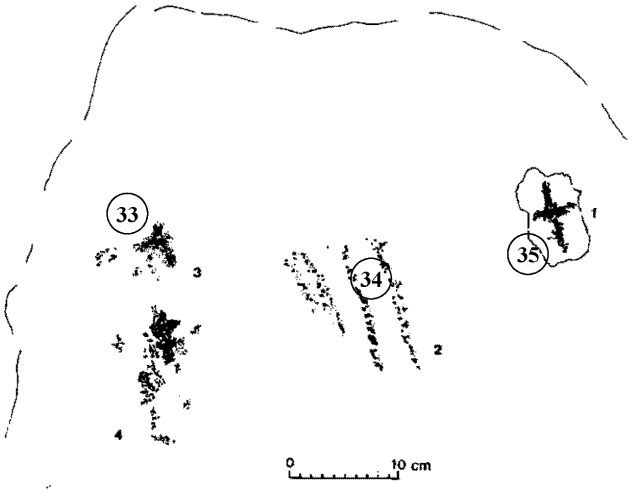

Figure S23. Sampled points on panel 1 in sector 3 of Barfaluy shelter (based on the tracing of the paintings presented in Figure 12 en [6])

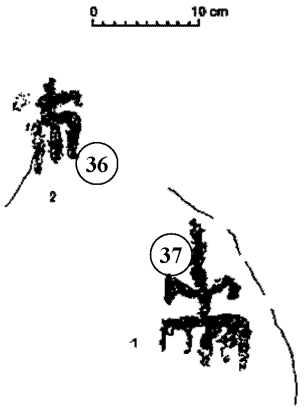

Figure S24. Sampled points in sector 1 of Barfaluy II shelter (based on the tracing of the paintings presented in Figure 9 in [6])

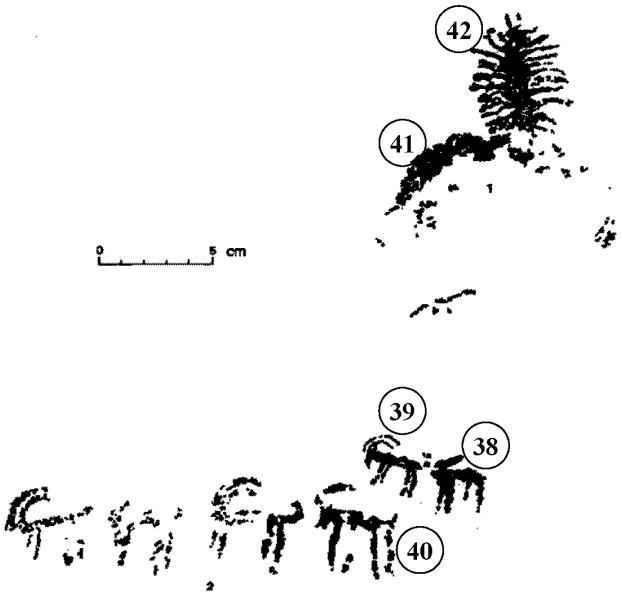

Figure S25. Sampled points in sector 1 of Barfaluy III shelter (based on the tracing of the paintings presented in Figure 17 in [6])

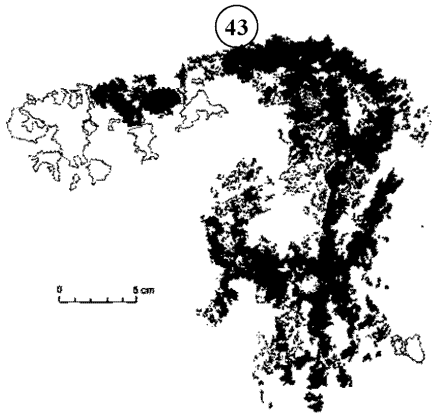

Figure S26. Sampled points in sector I of Barfaluy III shelter (based on the tracing of the painting presented in Figure 16 in [6])

Figure S27. Paintings on Quizans I shelter (based on the tracing of the paintings presented in Figure 2 in [7]).

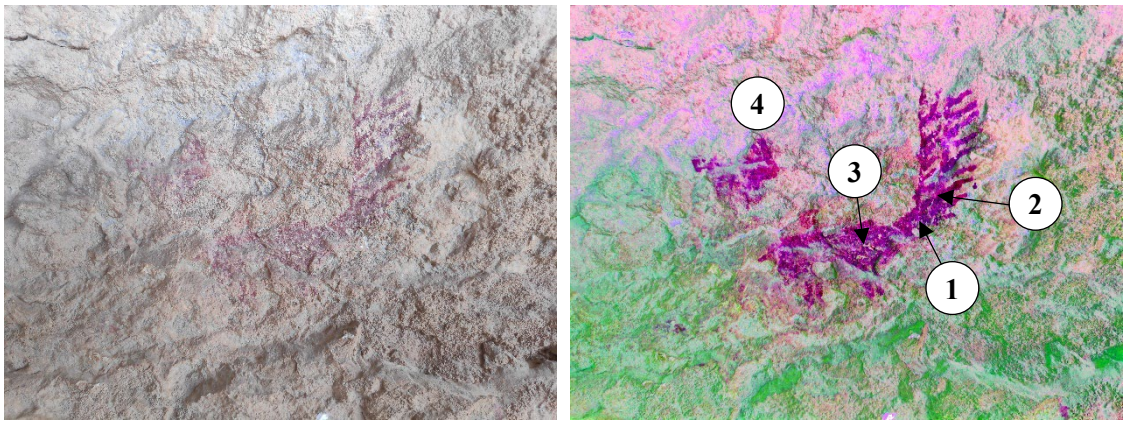

Figure S28. Sampled painting in Quizans I shelter (*left*: original photograph; *right*: after the application of a CRGB filter to facilitate visualization).

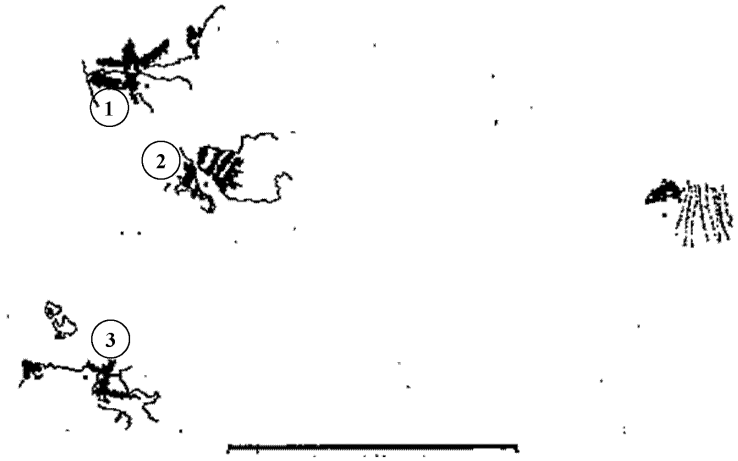

Figure S29. Sampled points in sector 1 of Lecina Superior shelter (based on the tracing of the paintings presented in Figure 3 in [8])

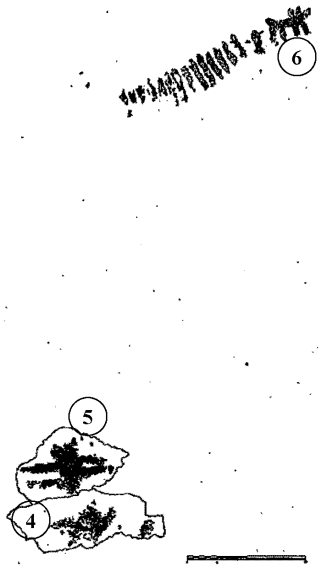

Figure S30. Sampled points in sector 2 of Lecina Superior shelter (based on the tracing of the paintings presented in Figure 6 in [8])

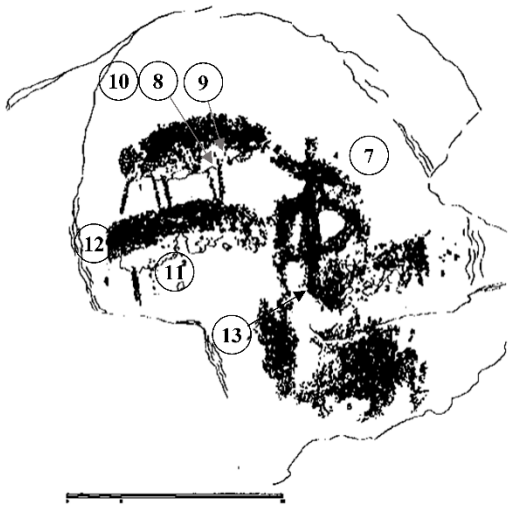

Figure S31. Sampled points in sector 3 of Lecina Superior shelter (based on the tracing of the paintings presented in Figure 7 in [8])

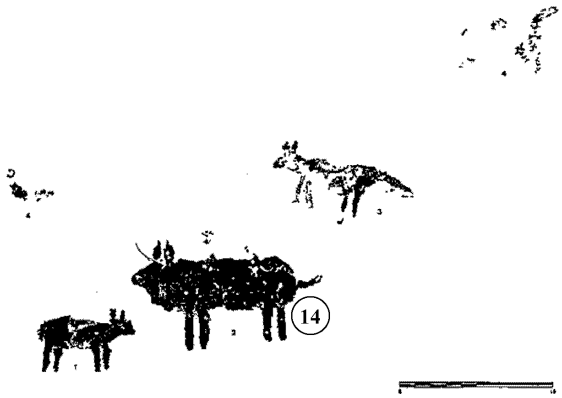

Figure S32. Sampled point in sector 5 of Lecina Superior shelter (based on the tracing of the paintings presented in Figure 9 in [8])

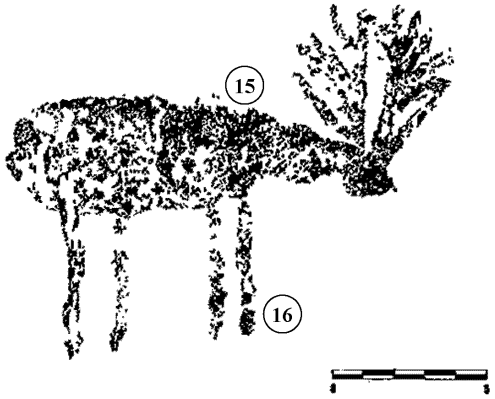

Figure S33. Sampled points in sector 6 of Lecina Superior shelter (based on the tracing of the painting presented in Figure 10 in [8])

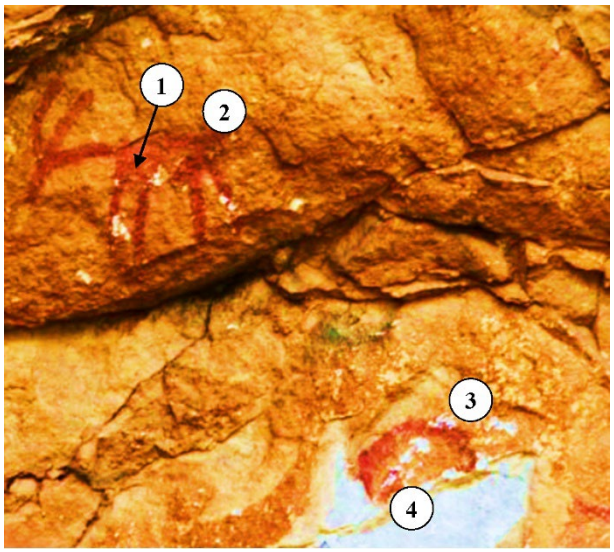

Figure S34. Sampled point in 'Covacho I' of Forau del Cocho shelter.

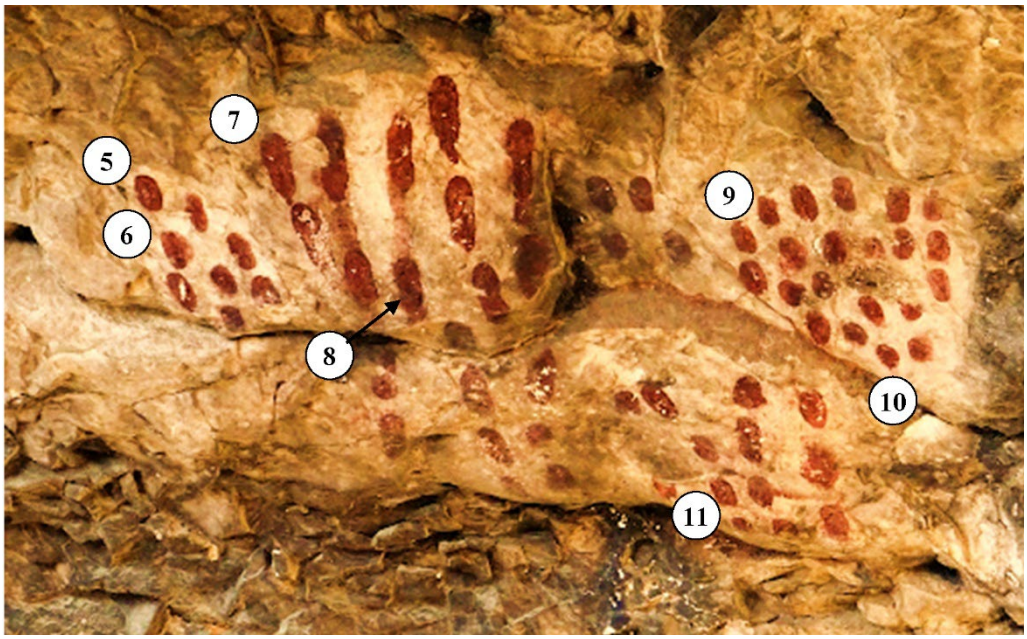

Figure S35. Sampled points in 'Covacho VIII' of Forau del Cocho shelter.

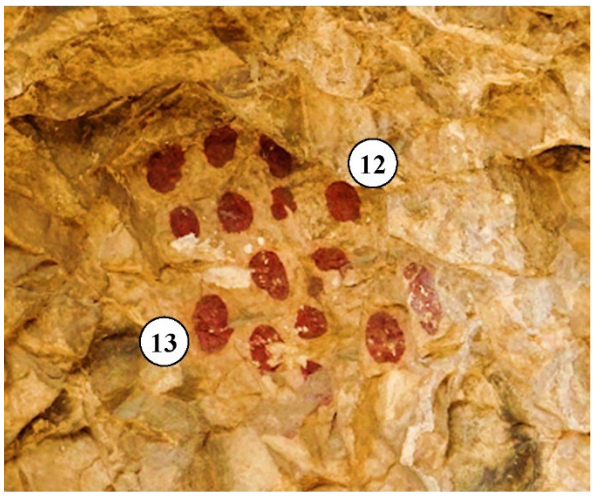

Figure S36. Sampled points in 'Covacho VIII' of Forau del Cocho shelter.

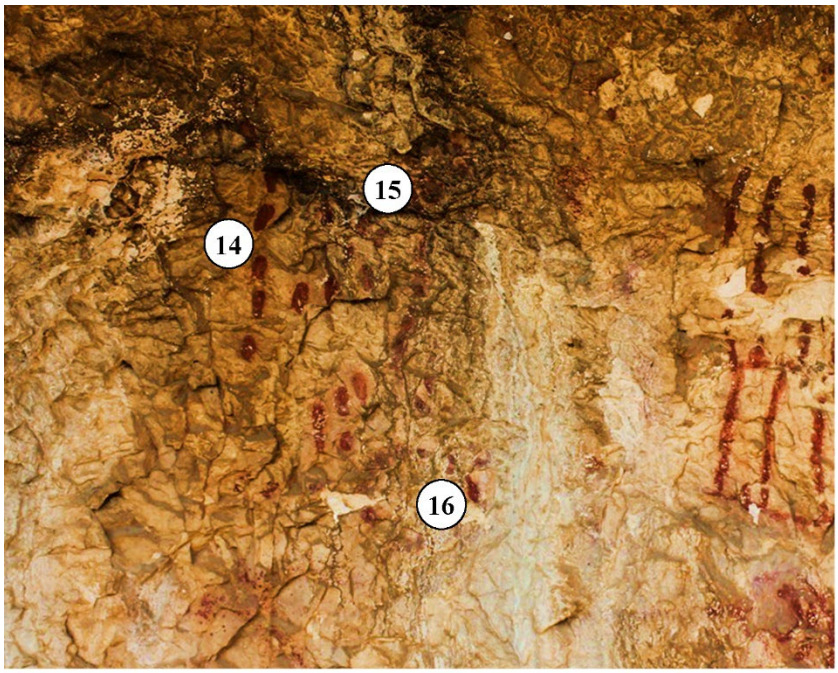

Figure S37. Sampled points in 'Covacho VII' of Forau del Cocho shelter.

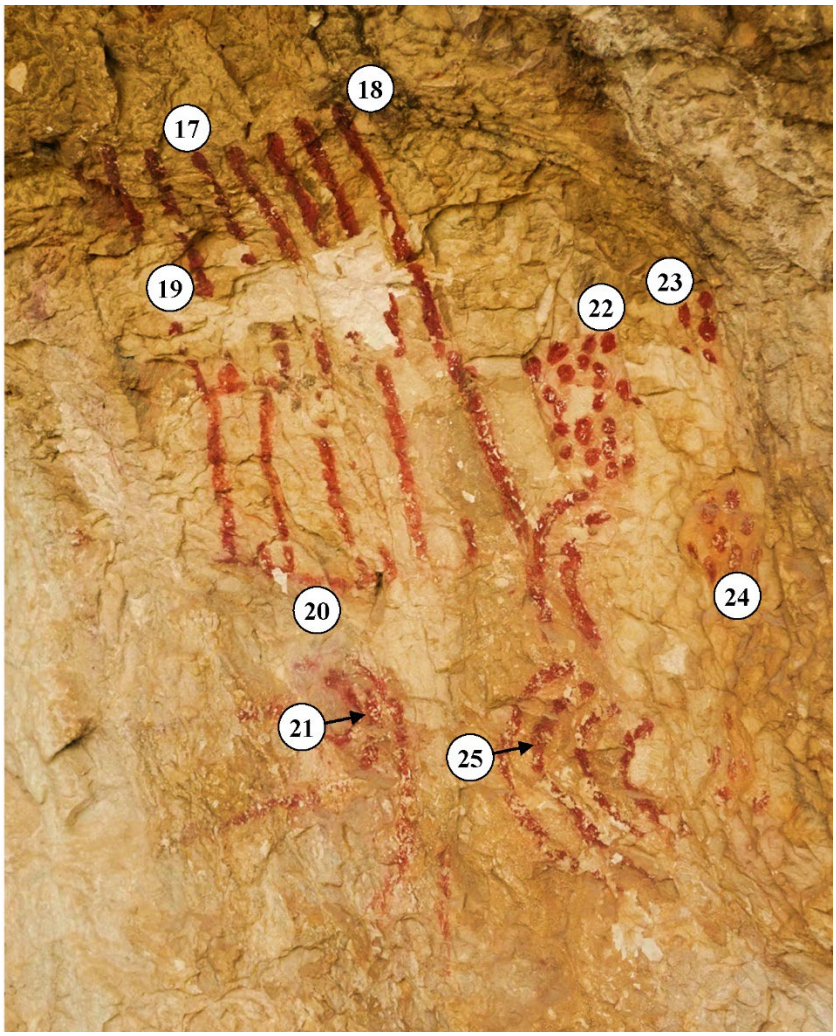

Figure S38. Sampled points in ‘Covacho VII’ of Forau del Cocho shelter.

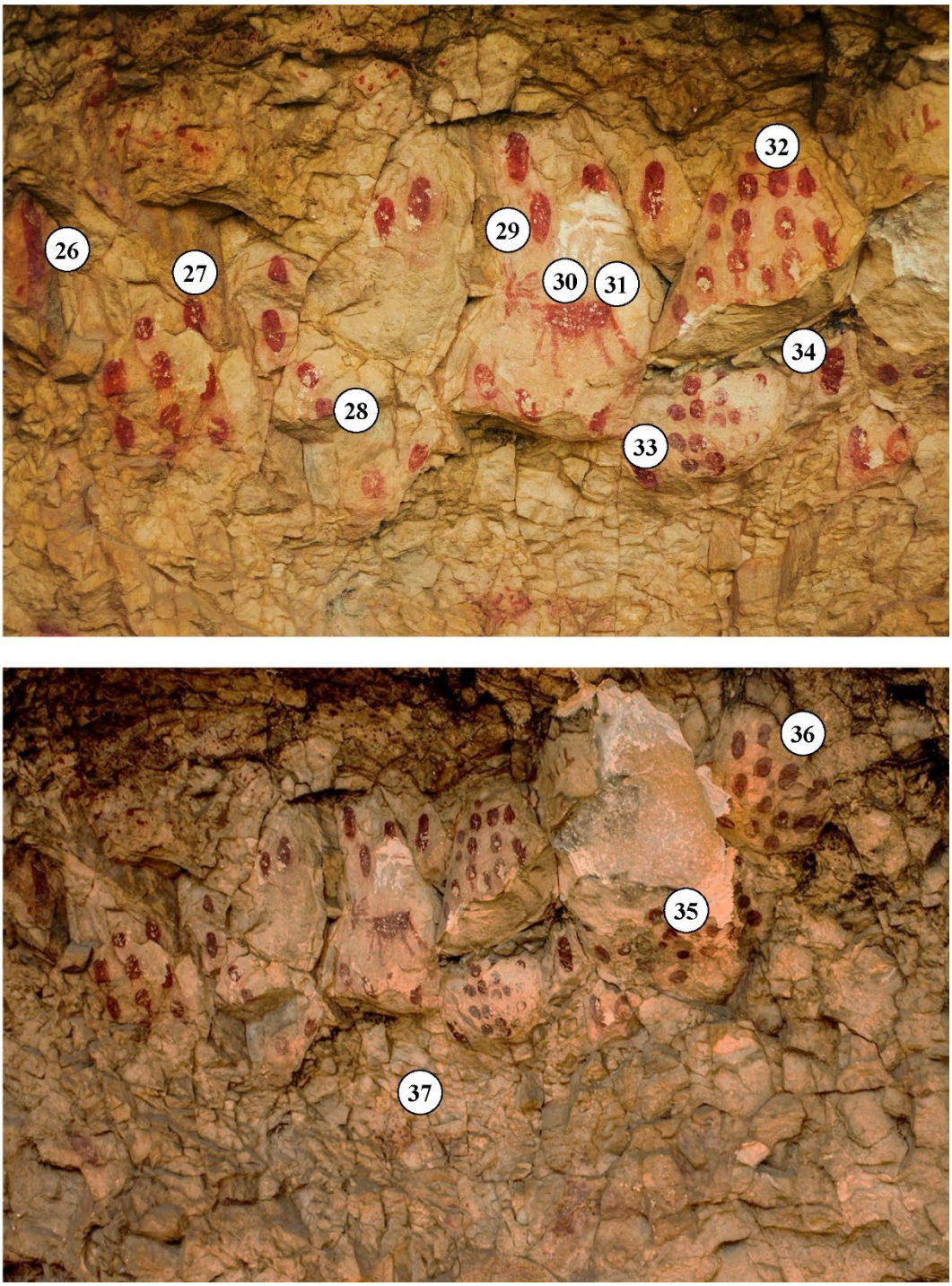

Figure S39. Sampled points in ‘Covacho VI’ of Forau del Cocho shelter.

Table S1. Chemical composition of the paintings of Muriecho shelter (in %) determined by pXRF.

Ref. point	Sector	*Bal* (C, N, O, F, Na)	Fe	Ti	Ca	Al	Si	P	S	Cl	K
1	A	54.41	5.23	0.04	23.03	0.89	2.17	0.35	13.29	0.09	0.41
2	A	56.86	2.30	0.04	27.94	1.01	2.68	0.18	8.50	0.11	0.31
3	A	56.81	3.20	0.05	27.05	0.91	2.40	0.20	8.89	0.11	0.32
4	A	52.81	4.10	0.04	25.57	0.79	2.09	0.18	13.93	0.09	0.33
5	A	49.96	4.00	0.04	26.91	1.01	2.32	0.16	14.31	0.08	0.35
6	A	48.97	2.69	0.06	27.66	1.04	2.41	0.24	16.44	0.07	0.34
7	A	50.07	3.48	0.06	27.39	1.60	3.58	0.31	12.88	0.09	0.44
8	A	50.84	2.40	0.06	28.59	1.43	3.48	1.01	10.60	0.11	0.44
9	A	55.41	4.27	0.07	24.38	0.81	2.54	0.61	11.16	0.07	0.57
10	A	53.79	2.45	0.06	27.94	1.10	2.83	0.10	11.26	0.08	0.35
11	A	55.30	2.50	0.07	27.66	0.92	2.84	0.73	9.28	0.09	0.50
Average	***Sector A***	*53.20*	*3.33*	*0.05*	*26.74*	*1.05*	*2.67*	*0.37*	*11.97*	*0.09*	*0.40*
12	B	51.98	3.12	0.08	27.81	0.99	2.92	0.61	11.96	0.07	0.37
13	B	46.89	3.24	0.07	25.56	1.00	2.41	0.25	20.08	0.04	0.38
14	B	42.72	2.59	0.06	28.30	1.17	2.69	0.35	21.59	0.08	0.38
15	B	43.45	2.15	0.06	26.14	0.80	1.87	0.32	24.75	0.05	0.34
16	B	45.11	3.00	0.06	24.97	0.86	1.97	0.29	23.24	0.04	0.39
17	B	45.04	8.10	0.07	24.39	1.04	2.15	0.19	18.48	0.07	0.39
18	B	49.36	3.49	0.05	24.16	0.40	1.45	0.16	20.55	0.05	0.28
Average	***Sector B***	*46.36*	*3.67*	*0.06*	*25.90*	*0.89*	*2.21*	*0.31*	*20.09*	*0.06*	*0.36*
19	C	47.65	2.04	0.10	25.13	1.52	3.93	0.47	18.48	0.04	0.50
20	C	45.99	3.35	0.06	23.72	1.00	2.25	0.44	22.73	0.04	0.38
21	C	42.19	3.42	0.06	24.94	1.24	3.06	0.12	24.43	0.05	0.37
22	C	47.90	2.26	0.10	27.76	2.48	5.50	1.03	11.52	0.10	0.60
Average	***Sector C***	*45.93*	*2.77*	*0.08*	*25.39*	*1.56*	*3.69*	*0.51*	*19.20*	*0.06*	*0.46*
23	D	51.04	1.79	0.08	30.09	1.79	4.33	1.62	8.55	0.12	0.46
24	D	51.39	5.25	0.09	25.50	1.60	4.21	1.15	9.88	0.10	0.59
25	D	48.69	3.01	0.10	26.19	1.63	4.12	0.76	13.84	0.11	0.63
26	D	51.37	1.78	0.10	27.84	1.99	4.79	0.84	10.41	0.15	0.63
27	D	56.67	2.18	0.08	25.98	1.34	3.83	1.24	7.97	0.07	0.50
28	D	44.65	2.07	0.07	26.56	1.53	3.44	0.61	20.43	0.05	0.46
29	D	44.36	1.89	0.07	26.30	1.49	3.34	0.64	21.33	0.06	0.42
30	D	45.65	2.47	0.07	24.92	1.93	3.99	0.47	19.88	0.06	0.48
31	D	51.67	1.92	0.10	25.09	1.12	3.13	0.72	15.03	0.06	0.44
32	D	49.49	3.80	0.10	25.09	2.11	4.86	0.66	12.93	0.07	0.68
33	D	47.57	0.90	0.10	25.17	1.88	4.18	0.41	19.05	0.05	0.60
Average	***Sector D***	*49.32*	*2.46*	*0.09*	*26.25*	*1.67*	*4.02*	*0.83*	*14.48*	*0.08*	*0.53*
Average	**Total**	*49.58*	*3.04*	*0.07*	*26.23*	*1.29*	*3.14*	*0.53*	*15.38*	*0.08*	*0.44*

Table S2. Chemical composition of the bedrock of Muriecho shelter (in %) determined by pXRF.

Ref. point	*Bal* (C, N, O, F, Na)	Fe	Ti	Ca	Al	Si	P	S	Cl	K
C1	56,59	-	0.05	41.03	-	0.60	-	1.64	0.04	-
C2	57,71	0.33	0.05	38.79	0.67	2.13	-	0.14	-	0.14

Table S3. Chemical composition of the paintings of Arpan shelter (in %) determined by pXRF.

Ref. point	Sector	*Bal* (C, N, O, F, Na)	Fe	Ti	Ca	Al	Si	P	S	Cl	K
1	1	56.69	0.89	0.06	34.42	1.36	4.29	-	1.73	0.15	0.35
2	1	53.69	1.49	0.10	29.57	1.30	5.03	0.55	7.49	0.12	0.63
3	1	58.05	2.98	0.06	27.62	1.71	6.42	1.36	1.22	0.09	0.41
4	1	45.49	1.07	0.04	29.10	0.52	1.20	0.20	22.14	0.03	0.17
5	1	58.20	2.01	-	31.29	0.68	3.46	0.32	3.67	0.09	0.21
6	1	58.41	0.97	0.03	31.51	0.52	4.90	0.13	3.22	0.09	0.17
7	1	58.77	1.62	0.04	31.01	0.43	2.61	0.10	5.09	0.08	0.17
8	1	59.22	1.05	0.05	34.57	0.55	2.15	0.18	1.84	0.12	0.24
9	3A/B	42.96	1.03	0.04	28.96	1.08	2.53	0.57	22.58	0.04	0.15
10	3A/B	51.41	5.85	0.06	22.69	0.44	1.68	0.12	17.10	0.09	0.44
11	3A/B	50.86	3.07	0.06	27.10	0.56	1.51	0.06	16.29	0.12	0.32
12	3A/B	50.23	1.30	0.09	27.44	1.27	3.67	-	15.22	0.13	0.51
13	3A/B	54.52	1.08	0.13	25.53	0.88	3.82	0.27	12.86	0.21	0.64
14	3C	43.91	6.54	0.03	24.22	0.85	1.55	0.37	22.21	0.05	0.19
15	3C	52.95	0.89	0.05	30.00	0.94	2.72	0.23	11.73	0.12	0.30
16	3D	55.32	4.97	0.04	28.28	0.79	2.95	0.67	6.44	0.17	0.31
17	3D	55.38	0.79	0.05	35.12	0.64	1.97	0.27	5.42	0.18	0.13
18	4	50.95	1.94	0.15	24.19	2.88	8.03	1.83	8.85	0.21	0.82
19	4	47.88	1.72	0.08	25.56	2.75	8.11	3.16	9.83	0.27	0.57
Average		52.89	2.17	0.06	28.85	1.06	3.61	0.61	10.26	0.12	0.35

Table S4. Chemical composition of the bedrock of Arpan shelter (in %) determined by pXRF.

Ref. point	*Bal* (C, N, O, F, Na)	Fe	Ti	Ca	Al	Si	P	S	Cl	K
C1	53.17	0.13	-	41.77	0.87	2.83	-	0.95	0.11	0.13
C2	50.09	0.08	0.03	39.54	0.47	1.36	0.09	8.11	0.06	0.10
C3	49.68	0.65	0.11	30.18	1.45	4.56	0.08	12.49	0.17	0.56
C4	50.54	0.85	0.12	26.18	1.59	5.06	0.55	14.23	0.16	0.66

Table S5. Chemical composition of the paintings of Mallata I and Mallata B1 shelters (in %) determined by pXRF

Mallata I											
Ref. point	**Sector**	***Bal* (C, N, O, F, Na)**	**Fe**	**Ti**	**Ca**	**Al**	**Si**	**P**	**S**	**Cl**	**K**
1	1	59.74	2.21	0.08	25.88	0.84	5.32	0.35	5.12	0.10	0.29
2	1	52.30	1.04	0.07	28.93	1.58	10.09	0.15	5.11	0.23	0.40
3	1	59.06	2.20	0.07	28.39	1.05	2.84	0.89	4.95	0.23	0.25
4	1	56.05	3.25	0.06	28.77	0.97	3.28	0.17	5.88	0.22	0.36
5	1	55.21	3.48	0.07	29.12	1.55	4.50	0.33	5.11	0.21	0.33
6	2	47.91	3.57	0.05	28.22	1.36	2.86	-	14.29	0.14	0.30
7	2	51.40	2.87	0.05	28.07	0.67	2.12	0.43	12.95	0.05	0.20
8	2	50.74	3.49	0.07	26.95	1.38	3.51	0.55	11.68	0.12	0.38
9	2	49.81	2.43	0.05	28.84	1.21	2.74	0.48	14.08	0.05	0.24
10	2	48.20	1.80	0.08	30.04	1.23	3.80	0.52	13.86	0.07	0.34
11	2	50.39	4.32	0.06	27.71	1.05	2.84	1.02	10.96	0.21	0.35
12	2	50.36	0.69	0.04	33.91	1.10	2.57	0.22	10.76	0.13	0.15
13	2	54.05	4.35	0.03	28.68	0.76	2.05	0.35	9.30	0.14	0.22
14	2	51.61	5.08	0.05	30.46	1.25	4.21	0.46	6.33	0.05	0.39
15	2	52.06	0.74	0.06	34.85	0.72	2.28	0.50	8.44	0.06	0.24
16	3	55.04	1.34	0.08	25.84	0.56	2.13	0.09	14.22	0.11	0.52
17	4	52.38	0.81	0.04	34.65	0.40	1.17	0.10	10.26	0.07	0.09
18	4	54.13	5.27	0.06	24.39	0.70	2.12	0.47	12.30	0.11	0.31
19	4	59.46	2.90	0.05	27.05	0.65	2.26	0.22	6.83	0.16	0.32
20	5	55.79	2.28	0.04	32.36	0.39	1.85	0.14	6.72	0.15	0.21
21	5	53.28	0.48	0.04	32.70	0.76	2.43	0.16	9.62	0.18	0.29
22	5	53.35	0.89	0.06	32.88	0.61	2.52	-	9.11	0.18	0.30
23	5	57.72	0.29	0.04	35.77	0.47	1.23	-	4.14	0.19	0.11
24	5	55.26	0.64	0.06	32.75	0.85	2.83	-	7.12	0.17	0.27
25	5	53.42	0.93	0.09	29.19	1.29	3.88	-	10.47	0.18	0.51
26	5	53.40	0.63	0.09	31.80	1.06	3.71	-	8.60	0.20	0.42
27	5	56.94	1.44	0.04	33.45	1.01	3.30	-	3.12	0.25	0.31
Average	***Mallata I***	*53.67*	*2.20*	*0.06*	*30.06*	*0.94*	*3.13*	*0.38*	*8.94*	*0.15*	*0.30*
Mallata B1											
Ref. point	**Sector**	***Bal* (C, N, O, F, Na)**	**Fe**	**Ti**	**Ca**	**Al**	**Si**	**P**	**S**	**Cl**	**K**
28	1	61.77	6.78	0.05	25.75	0.51	1.68	0.06	2.76	0.14	0.43
29	1	55.87	8.61	-	26.18	0.67	1.77	-	6.40	0.14	0.21
30	1	58.21	4.87	-	31.01	0.63	1.93	-	2.97	0.16	0.13
31	1	62.72	3.22	-	29.25	0.39	1.61	-	2.32	0.09	0.32
32	1	55.67	1.82	-	31.96	0.71	5.17	-	2.07	0.27	0.28
33	1	57.94	10.58	-	26.13	0.75	2.08	-	1.84	0.25	0.25
34	1	54.28	1.56	-	35.85	0.98	2.49	-	3.09	0.14	0.18
35	1	55.52	5.08	0.03	30.77	0.63	4.50	-	2.51	0.37	0.50
36	1	58.24	6.63	0.04	22.77	1.01	3.31	0.55	6.94	0.12	0.27
37	2	50.64	4.85	0.09	27.04	2.98	7.17	0.63	5.72	0.12	0.59
38	2	54.71	1.29	-	34.16	0.60	1.74	-	7.08	0.13	0.19
39	2	59.24	1.12	0.03	33.82	0.37	1.28	-	3.85	0.09	0.15
40	3	61.22	0.53	-	28.62	0.32	2.03	0.07	6.85	0.13	0.16
41	3	47.55	9.98	0.03	27.39	0.51	2.09	0.17	11.87	0.09	0.19
42	3	57.74	2.18	0.04	29.59	0.96	3.17	-	5.77	0.18	0.29
Average	***Mallata B1***	*56.75*	*4.61*	*0.04*	*29.35*	*0.80*	*2.80*	*0.30*	*4.80*	*0.16*	*0.28*
Average	**Total**	54.77	3.06	0.06	29.81	0.89	3.01	0.36	7.46	0.15	0.29

Table S6. Chemical composition by pXRF of the paintings of Barfaluy shelters (in %).

Ref. point	Sector	*Bal* (C, N, O, F, Na)	Fe	Ti	Ca	Al	Si	P	S	Cl	K
1	I.1	64.13	3.09	0.17	27.21	0.67	2.60	-	0.82	0.08	0.46
2	I.1	63.65	1.58	0.08	30.94	0.34	1.54	-	1.42	0.09	0.26
3	I.1	63.12	0.50	0.05	31.74	0.36	1.58	-	2.39	0.09	0.13
4	I.1	47.16	0.29	0.07	43.45	1.83	3.76	0.16	2.94	0.11	0.19
5	I.1	51.56	0.45	0.05	37.57	1.07	2.91	0.24	4.81	0.08	0.21
6	I.1	56.76	2.33	0.12	32.88	1.09	3.41	0.19	2.76	0.07	0.34
7	I.1	58.91	0.19	0.03	35.50	0.70	2.01	-	2.42	0.09	0.10
8	I.1	54.20	1.10	0.11	34.49	1.73	3.84	0.16	3.94	0.09	0.28
9	I.1	56.52	1.81	0.10	34.75	1.08	3.38	-	1.86	0.06	0.31
10	I.1	55.22	1.04	0.08	35.13	1.62	3.55	0.06	2.94	0.06	0.24
11	I.1	57.45	1.71	0.12	31.04	1.52	3.81	-	2.10	0.06	0.38
12	I.1	55.87	1.77	0.14	33.78	1.37	3.58	0.14	2.93	0.06	0.31
13	I.1	57.26	1.13	0.14	32.74	1.34	4.19	0.24	2.45	0.06	0.39
14	I.1	56.47	0.42	0.11	34.46	1.17	3.06	-	3.92	0.04	0.30
15	I.1	58.71	0.47	0.11	33.37	0.78	3.44	-	2.75	0.05	0.30
16	I.1	59.79	1.28	0.09	33.05	0.53	1.61	-	3.37	0.06	0.18
17	I.1	60.13	0.28	0.06	32.11	0.36	1.57	-	5.23	0.07	0.15
18	I.2	56.60	0.24	0.07	32.44	-	1.57	-	8.83	0.06	0.15
– [a]	I.3	57.76	0.19	0.07	32.80	0.35	1.60	-	5.82	0.07	0.11
19	I.3	48.54	0.31	0.08	39.71	0.69	1.98	0.15	8.19	0.09	0.19
20	I.3	56.49	0.39	0.07	33.12	0.38	1.59	0.16	7.52	0.10	0.14
Average	***Barf. I***	*56.97*	*0.98*	*0.09*	*33.92*	*0.95*	*2.69*	*0.17*	*3.78*	*0.07*	*0.24*
21	II	52.40	3.53	0.08	27.22	1.44	4.42	0.47	9.65	0.15	0.52
22	II	55.08	4.28	0.06	24.84	-	1.37	0.20	13.45	0.06	0.25
23	II	46.55	3.26	0.09	26.44	1.47	3.58	0.50	17.49	0.07	0.44
24	II	52.72	3.21	0.05	30.62	0.41	1.42	-	9.98	0.15	0.24
25	II	51.77	2.79	0.06	29.26	0.33	1.57	-	13.84	0.06	0.22
26	II	51.75	2.06	0.06	31.90	0.36	1.77	0.10	11.66	0.06	0.17
27	II	56.91	4.53	0.05	27.97	-	1.00	-	7.77	0.10	0.25
28	II	58.84	0.99	0.16	27.72	0.81	3.15	0.09	7.68	0.14	0.37
29	II	56.93	4.41	0.07	28.50	0.39	1.67	-	7.57	0.04	0.25
30	II	56.66	4.26	0.04	27.91	0.50	1.36	-	8.70	0.12	0.27
31	II	48.50	3.27	0.06	28.20	0.78	1.42	0.12	17.19	0.05	0.27
32	II	58.50	4.02	0.07	27.13	0.54	1.83	0.30	6.90	0.20	0.35
33	II	50.56	3.94	0.05	27.98	0.78	2.38	0.17	13.66	0.05	0.25
34	II	52.71	0.40	0.06	34.95	0.57	2.38	-	8.37	0.24	0.20
35	II	56.44	1.77	0.06	31.37	0.60	1.91	0.17	6.35	0.06	0.17
– [b]	II	53.35	0.70	0.08	32.29	1.08	2.61	0.35	9.04	0.13	0.32
– [c]	II	53.94	0.40	0.09	33.66	0.72	2.38	0.09	8.36	0.10	0.21
36	II.1	53.54	0.45	0.09	30.15	0.57	2.93	0.24	10.07	0.12	0.30
37	II.1	52.15	0.92	0.15	26.20	1.25	5.41	0.43	12.72	0.09	0.58
Average	***Barf. II***	*55.43*	*1.73*	*0.08*	*31.72*	*0.86*	*2.53*	*0.21*	*6.92*	*0.09*	*0.27*
38	III	64.04	0.35	0.08	28.46	0.87	2.91	-	2.81	0.13	0.31
39	III.2	59.06	0.36	0.08	31.12	0.96	3.68	0.20	3.98	0.17	0.32
40	III.2	59.00	0.35	0.08	29.28	1.14	4.14	0.12	5.29	0.16	0.36
41	III.2	61.98	0.22	0.07	30.57	0.53	2.07	-	4.23	0.14	0.18
42	III.2	63.77	0.22	0.06	30.31	0.50	1.98	-	2.78	0.15	0.19
43	III.1	57.49	0.14	0.05	35.27	0.27	1.03	-	5.18	0.27	0.29
Average	***Barf. III***	*60.89*	*0.27*	*0.07*	*30.84*	*0.71*	*2.64*	*0.16*	*4.05*	*0.17*	*0.28*
Average	**Total**	56.11	1.55	0.08	31.56	0.83	2.54	0.21	6.61	0.10	0.27

[a] Seated idol, not shown in the tracings of the paintings.
[b-c] Vertical stain in panel 1, sector 3, not shown in tracings of the paintings.

Table S7. Chemical composition of the bedrock of Barfaluy shelters (in %) determined by pXRF.

Ref. point	*Bal* (C, N, O, F, Na)	Fe	Ti	Ca	Al	Si	P	S	Cl	K
C1	56.58	0.11	0.05	35.91	0.57	2.31	0.08	3.23	0.05	0.14
C2	43.32	0.05	0.04	40.66	0.41	1.14	-	14.18	0.03	0.09

Table S8. Chemical composition of the paintings of Lecina Superior shelter (in %) determined by pXRF.

Ref. point	Sector	*Bal* (C, N, O, F, Na)	Fe	Ti	Ca	Al	Si	P	S	Cl	K
1	1	60.16	4.44	0.07	25.94	1.21	3.94	0.94	1.50	0.09	0.51
2	1	56.92	6.33	0.09	24.54	1.65	5.30	1.97	1.24	0.08	0.54
3	1	57.48	1.91	0.06	31.11	1.24	3.84	0.58	2.08	0.05	0.44
4	2	59.54	1.67	0.03	33.92	0.63	2.04	0.11	1.66	0.08	0.24
5	2	58.60	0.93	0.06	32.57	0.60	2.65	0.22	3.91	0.10	0.29
6	2	57.40	0.23	0.06	34.83	0.94	3.92	0.06	2.13	0.09	0.29
7	3	48.48	2.76	0.10	28.46	1.86	5.48	0.07	10.89	0.08	0.61
8	3	53.54	0.05	-	29.32	0.43	1.51	-	14.88	0.09	0.08
9	3	52.54	0.13	0.04	29.91	0.69	2.37	-	13.99	0.10	0.17
11	3	51.93	0.09	0.04	27.95	1.05	3.22	0.06	14.30	0.09	0.13
12	3	49.59	0.11	0.03	29.65	0.27	1.52	-	18.57	0.09	0.12
13	3	53.19	0.29	0.04	31.35	-	1.70	-	11.92	0.13	0.15
14	5	54.79	0.64	0.10	30.00	1.82	6.19	0.67	4.04	0.10	0.57
15	6	61.51	0.14	0.05	34.19	0.50	1.86	-	1.39	0.07	0.21
16	6	59.58	0.25	0.06	31.95	0.87	2.99	0.10	3.78	0.11	0.26
– [a]	6	60.40	0.47	0.06	30.87	0.52	2.53	-	4.77	0.06	0.24
Average		55.98	1.21	0.06	30.06	0.95	3.19	0.48	7.07	0.09	0.29

[a] Orange pigment, not natural, on the left in sector 5, not shown in the tracings of the paintings.

Table S9. Chemical composition of the bedrock of Lecina superior shelter (in %) determined by pXRF.

Ref. point	*Bal* (C, N, O, F, Na)	Fe	Ti	Ca	Al	Si	P	S	Cl	K
C1	47.83	0.14	0.03	36.44	0.40	2.05	0.16	12.07	0.37	0.45
C2	58.99	-	-	36.33	-	2.95	0.11	1.34	0.06	0.13
C3	46.53	0.04	-	44.80	0.61	1.44	-	6.45	0.02	0.04

Table S10. Chemical composition of the paintings of Forau del Cocho shelter (in %) determined by pXRF.

Ref. point	'Covacho'	*Bal* (C, N, O, F, Na)	Fe	Ti	Ca	Al	Si	P	S	Cl	K
1	I	53.19	0.76	0.07	30.96	1.49	4.49	0.95	7.69	0.06	0.29
2	I	52.76	1.01	0.09	27.64	1.55	4.80	0.43	11.18	0.08	0.38
3	I	48.98	0.56	0.05	28.42	0.68	2.70	0.59	17.68	0.05	0.25
4	I	46.90	0.53	0.05	28.73	0.97	3.13	0.17	19.15	0.05	0.29
*	I	45.41	0.70	0.05	32.88	0.80	2.44	0.25	17.11	0.08	0.22
5	VIII	54.31	7.69	0.05	22.11	0.77	2.66	0.26	10.16	0.18	0.26
6	VIII	46.59	10.81	0.04	25.39	1.03	2.25	0.14	11.70	0.18	0.22
7	VIII	59.78	7.72	0.04	23.12	0.40	1.79	0.08	6.65	0.12	0.23
8	VIII	56.66	4.46	0.05	26.49	0.77	3.07	1.11	5.74	0.17	0.33
9	VIII	56.80	8.55	0.03	25.66	0.52	1.65	-	6.38	0.15	0.20
10	VIII	48.93	6.36	0.04	28.10	1.26	2.92	0.42	11.54	0.19	0.18
11	VIII	54.26	6.01	-	29.80	0.61	2.34	0.13	6.39	0.15	0.21
12	VIII	51.27	2.18	0.05	28.80	0.70	1.98	0.06	14.58	0.11	0.21
13	VIII	51.86	2.32	0.05	27.78	0.68	2.32	0.21	14.41	0.11	0.22
14	VII	58.62	1.70	0.04	31.01	0.92	2.79	-	4.29	0.26	0.26
15	VII	57.50	1.09	0.04	26.98	0.55	1.64	-	11.72	0.22	0.23
16	VII	51.08	0.89	0.07	31.71	1.65	4.12	0.44	8.16	0.22	0.32
17	VII	53.06	4.05	0.03	27.82	0.68	1.69	-	12.23	0.18	0.14
18	VII	63.12	3.42	0.03	27.86	0.62	2.19	-	2.28	0.22	0.21
19	VII	53.62	0.64	0.04	33.16	0.30	1.14	0.51	10.23	0.15	0.15
20	VII	50.88	0.63	0.05	32.52	0.63	1.91	0.07	12.90	0.14	0.23
21	VII	50.07	1.31	0.06	29.30	1.77	4.53	1.01	10.04	0.31	0.33
22	VII	56.29	2.22	0.04	29.47	0.73	2.48	0.30	8.10	0.16	0.18
23	VII	47.26	1.79	0.06	30.87	1.40	3.70	0.34	13.91	0.23	0.39
24	VII	53.54	1.70	0.07	29.61	1.32	3.75	0.32	9.01	0.20	0.43
25	VII	58.22	1.87	0.06	24.01	0.71	2.74	0.13	11.59	0.18	0.43
26	VI	53.03	2.34	0.08	26.77	0.97	3.89	0.11	12.14	0.19	0.43
27	VI	46.53	1.99	0.04	30.47	0.94	2.28	0.28	17.03	0.19	0.18
28	VI	46.58	1.36	0.05	31.02	0.57	1.92	-	18.17	0.13	0.17
29	VI	50.71	1.01	0.03	30.41	0.27	1.25	-	15.99	0.13	0.17
30	VI	44.89	1.27	0.06	30.50	0.96	2.61	-	19.30	0.12	0.27
31	VI	43.60	1.54	0.05	29.84	0.81	2.01	0.09	21.72	0.09	0.18
32	VI	51.44	1.88	0.05	29.75	1.28	2.88	0.22	11.91	0.28	0.23
33	VI	43.36	4.29	0.05	27.58	0.58	2.03	0.23	21.44	0.09	0.28
34	VI	46.46	2.59	0.05	27.39	0.90	2.59	0.50	16.40	0.12	0.24
35	VI	49.28	1.88	0.03	27.60	0.66	1.80	0.35	18.15	0.09	0.11
36	VI	51.34	0.99	0.06	31.92	0.79	4.05	-	10.41	0.19	0.20
37	VI	47.96	1.24	0.06	30.84	1.14	2.62	0.21	15.42	0.13	0.34
Average		51.48	2.72	0.05	28.80	0.88	2.66	0.34	12.44	0.15	0.25

* Small dots not shown in the photograph.

Table S11. Chemical composition of the bedrock of Forau del Cocho shelter (in %) determined by pXRF.

Ref. point	*Bal* (C, N, O, F, Na)	Fe	Ti	Ca	Al	Si	P	S	Cl	K
C1	49.33	0.19	0.06	32.03	0.73	1.92	-	15.29	0.22	0.19

Principal Component Analysis Results

When calcium was excluded as a common factor of the support, as well as titanium and chlorine (minority elements that did not help to discriminate), 84.6% of the variance was explained by three factors. The parameters of specific extracted initial communalities were checked by the Kaiser–Mayer–Olkin (KMO) test and the Bartlett test of sphericity to test data rationality and sampling adequacy of the analysis. The KMO value of 0.579 (>0.5) revealed sufficient sampling, and the significance level from the Bartlett test <0.0001 indicated that the data were appropriate and useful to substantially reduce the data dimension. Factor F1 (which accounted for 50.14% of the total cumulative variance) was linked to Al, Si, P, and K, i.e., to components of clay; factor F2 (which explained 18.47% of the variance) consisted of S, and factor F3 (which explained 16.0% of the total cumulative variance) was linked to Fe. In the F1 vs. F2 plot (Figure S40a), it may be observed that the measurements from some shelters appear as clusters, in such a way that Barfaluy measurements (black) are concentrated in the lower left corner, Muriecho (fuchsia) in the upper right corner, and Chimiachas-Forau del Cocho-Quizans in the intermediate zone. On the other hand, Mallata and Arpan's measurements are scattered. This mainly points to differences in the bedrock composition. Conversely, the F3 factor (associated with iron) did not allow for pigment discrimination among shelters (Figure S40b).

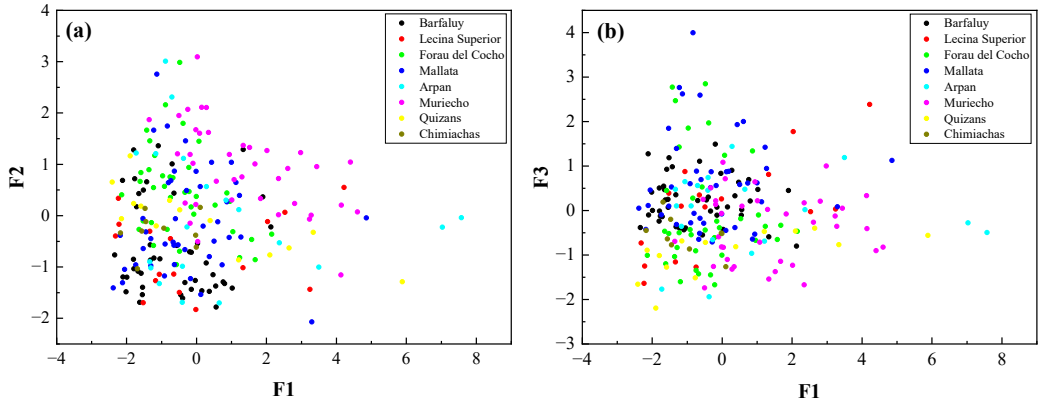

Figure S40. (**a**) F2 vs. F1 biplot; (**b**) F3 vs. F1 biplot.

References (reference numbers do not match those that appear in the main document)

1. Baldellou, V.; Ayuso, P.; Painaud, A.; Calvo, M.J. Las pinturas rupestres de la partida de Muriecho (Colungo y Bárcabo, Huesca). *Bolskan: Revista de arqueología del Instituto de Estudios Altoaragoneses* **2000**, 33-86.
2. Baldellou, V.; Painaud, A.; Calvo, M.J.; Ayuso, P. Las pinturas rupestres del barranco de Arpán (Asque-Colungo, Huesca). *Bolskan: Revista de arqueología del Instituto de Estudios Altoaragoneses* **1993**, 31-96.
3. Baldellou, V.; Painaud, A.; Calvo, M.J. Las pinturas esquemáticas del Tozal de Mallata (Asque-Colungo. Huesca). *Zephyrus: Revista de prehistoria y arqueología* **1983**, 123-129.
4. Painaud Guillaume, A.; Ayuso, P. Algunas reflexiones sobre una nueva figura en el abrigo de Mallata I (Asque, Colungo, Huesca). *Bolskan: Revista de arqueología del Instituto de Estudios Altoaragoneses* **2019**, 23-30.
5. Baldellou, V.; Painaud, A.; Calvo, M.J. Las pinturas esquemáticas de Mallata B (Huesca). *Boletín del Museo de Zaragoza* **1985**, 17-36.
6. Baldellou, V.; Painaud, A.; Calvo, M.J.; Ayuso, P. Las pinturas esquemáticas de la partida de Barfaluy (Lecina-Bárcabo. Huesca). *Empúries* **1986**, 64-83.
7. Baldellou, V.; Painaud, A.; Calvo, M.J. Las pinturas esquemáticas de Quizáns y Cueva Palomera (Alquézar. Huesca. *Zephyrus: Revista de prehistoria y arqueología* **1983**, 117-122.
8. Baldellou, V.; Painaud, A.; Calvo, M.J. Los covachos pintados de Lecina Superior, del Huerto Raso y de la Artica del Campo (Huesca). *Bolskan: Revista de arqueología del Instituto de Estudios Altoaragoneses* **1988**, 147-174.